January 2011

# Investigating Contributions Of Langerhans Cells To The Epidermal Oxidative Stress Response

Debra Smith

# Investigating Contributions of Langerhans Cells to the Epidermal Oxidative Stress Response

A Thesis Submitted to the

Yale University School of Medicine

In Partial Fulfillment of the Requirements for the

Degree of Doctor of Medicine

By

Debra A. Smith

2011

INVESTIGATING THE CONTRIBUTIONS OF LANGERHANS CELLS TO THE EPIDERMAL OXIDATIVE STRESS RESPONSE. Debra A. Smith, Julia Lewis, Renata Filler, Kseniya Golubets, Michael Girardi. Department of Dermatology, Yale University, School of Medicine, New Haven, CT.

Langerhans cells (LC) play an essential role in the development of skin cancer in a chemical carcinogenesis mouse model. To elucidate the mechanism of this effect, LC-deficient (Langerin-dipheria toxin A or human Langerin-diphtheria toxin receptor transgenic) mouse epidermis was compared to normal littermate controls (NLC) to assess whether levels of oxidative stress or DNA damage are affected by LC. Groups of mice were treated with either ultraviolet B (UVB) irradiation or 7,12-dimethylbenz(a)anthracene (DMBA)/tetradecanoylphorbol-13-acetate (TPA) carcinogens. Immunofluorecent staining with 8oxoguanine was used as a quantitative marker of oxidative stress and γH2AX staining was used to assess double stranded DNA breaks (DSB). Multiple consecutive high power fields assessed using a confocal microscope (Zeiss 510 META LSM) were quantified with ImageJ software (NIH).

These experiments represent a novel assay for assessing oxidative stress and DSB in epidermal sheets. LC-deficient epidermis exposed to UVB irradiation had higher levels of both oxidative stress (179.2±13.6 in LC-deficient, 96.3±27.6 in NLC; $p=1.04x10^{-4}$) and DSB (40.86±3.6 in LC-deficient, 25.00±2.2 in NLC; p=0.005) than LC-intact controls, suggesting that LC may protect against UVB-induced oxidative stress and DNA damage. DMBA treated LC-deficient epidermis had a greater number of DSB compared to LC-intact controls (62.82±3.0 in LC-deficient, 81.15±3.8 in NLC; p=0.005),

suggesting the LC promote DMBA-induced DNA damage. A more thorough understanding of the role of LC in carcinogenesis may have important implications in both cancer prevention and the development of potential immunotherapies.

**Acknowledgements**

I am forever grateful to my parents, Doris and Donald Smith, for their unconditional love and support. I would also like to thank the people of the Yale University School of Medicine, including the institution's faculty, staff and my classmates. My research mentor, Dr. Michael Girardi and the members of his laboratory, Julia Lewis, Renata Filler, and Kseniya Golubets all provided indispensable guidance and patience; I could not have pursed this project without their help. Lastly, I would like to acknowledge and thank the Office of Student Research for providing multiple short term funding grants without which I could not have conducted this research.

# Table of Contents

## List of Figures

# Introduction

## I. Langerhans Cells:

Epithelial tissues exist at the critical interface between the body and the environment where they repeatedly encounter DNA-damaging chemical compounds and other mutagens. Therefore it is not surprising that the majority of cancers and cancer-related deaths result from epithelium-derived carcinomas including the skin, lung, colon and GU tract. According to the cancer immunosurveillance hypothesis, cancer cells express mutated proteins that can allow the immune system to identify and destroy transformed cells before they evolve into a discernable tumor (1). The importance of the immune system in protecting against carcinogenesis is apparent given the increased susceptibility of immunosuppressed populations, such as organ transplant recipients (2). Furthermore, mice deficient in gamma-delta T cells are more susceptible to early papilloma formation (3). The interaction between the immune system and tumor cells is more complicated, however, as there is evidence that some components of the immune system may actually promote, rather than protect against carcinogenesis. Recent investigations in the Girardi laboratory have demonstrated that 1) mice deficient in the epidermal dendritic cell population, called Langerhans cells, are protected against chemically induced cutaneous carcinogenesis (4), and 2) a perforin deficient subset of $CD8^+$ alpha-beta T cells has been implicated in increased tumor incidence and progression to carcinoma (3, 5). This raises the important question: Can we clinically

enhance the aspects of the immune system that protect against carcinogenesis while diminishing the tumorgenic components of the immune system?

Epithelial murine and human tissue contains constitutively associated immune cells. Notably, in mouse skin there is a unique population of immature dendritic cells called Langerhans cells (LC) and dendritic epithelial T cells (gamma-delta T cells). In fact, the epidermis represents one of the largest T cell compartments in the body. These immune cells are situated in an ideal location for immunosurveillance and ablation of potential developing tumors in the skin. During the steady state, LC are important in surveying the skin and collecting antigens. Upon stimulation by inflammatory signals, LC rapidly change shape and increase expression of MHC II molecules as well as co-stimulatory molecules and selected chemokine receptors. Additionally, they migrate to draining lymph nodes where they present antigens collected in the skin and express co-stimulatory molecules instrumental in activating T cells and initiating the adaptive arm of the immune response (6, 7). In light of these activities of LC, it has been presumed that LC should contribute to the immune fight against carcinogenesis by presenting tumor antigens to T cells and therefore activating an immuno-protective response. Surprisingly, recent studies show that in a two-stage chemical carcinogenesis model, LC actually contribute to the development of tumors. In fact, LC-deficient mice are virtually incapable of forming papillomas in this model (4). This finding has important implications as many immunotherapy regimens seek to directly activate dendritic cell populations.

Polyaromatic hydrocarbons, such as 7,12-dimethylbenz(a)anthracene (DMBA), are a mutagenic class of molecules shown to cause DNA adduct formation and oxidative

stress induced-DNA mutations (8). These compounds are found in tobacco smoke implicated in lung cancer, smoked and charbroiled meat implicated in colon cancer, ambient pollution, and industrial waste (9). Treatment of murine skin with DMBA followed by repeated exposure to low dose tetradecanoylphorbol-13-acetate (TPA), a phorbol ester which promotes low-grade inflammation, models what is observed in many human cancers and results in the development of papillomas and carcinomas. Using this model of chemical carcinogenesis, investigations in the Girardi laboratory have demonstrated that even with high doses of mutagen and promoter in a highly susceptible strain (FVB), LC-deficient mice remained tumor-free at 7 weeks, at which time all wild-type mice had multiple tumors. Further unpublished studies in the Girardi laboratory show that mice deficient in LC treated with the DMBA chemical carcinogen are more resistant to developing mutations in the H-ras proto-oncogene. This H-ras mutation is associated with malignant progression and is found in greater than 94% of DMBA-induced papillomas (10). Clearly, under certain conditions, LC may facilitate mutagenesis and tumor development. Investigation into mechanism through which LC promote carcinogenesis is essential to the development of more effective methods of prevention and treatment.

**II. Oxidative Stress:**

A recurring theme connecting populations of immune cells and carcinogenesis is the association between chronic inflammatory conditions and the development of cancer. For example, inflammatory bowel disease is associated with colon cancer, reflux esophagitis increases the risk of adenocarcinoma (Barrett's esophagus), hepatitis

predisposes to liver cancer, schistosomiasis is associated with bladder cancer, chronic Helicobacter pylori infection leads to gastric cancer, and chronic sun exposure is associated with skin cancer. This association may be explained by oxidative stress.

Oxidative and nitrative stress are caused by an imbalance in the production of reactive species and the biological system's ability to detoxify the reactive intermediates and repair resulting damage (11). Macrophages and neutrophils release large amounts of genotoxic reactive oxygen species (ROS) and reactive nitrogen species (RNS) in a "respiratory burst" as an essential part of innate immunity to pathogens (12). Inflammatory cells and cancer cells produce free radicals and soluble mediators such as metabolites of arachidonic acid, cytokines and chemokines, which further produce reactive species. These, in turn strongly recruit inflammatory cells in a vicious cycle. Reactive intermediates of oxygen and nitrogen may directly oxidize DNA or interfere with mechanisms of DNA repair in addition to damaging proteins, carbohydrates and lipids, thus contributing to the progression of carcinogenesis (13).

Guanine is the most easily oxidized among the four DNA bases. ROS induce the formation of 8-oxoguanine (8-oxoG), one of the most common and specific mutations associated with oxidative stress. If it is not repaired, this DNA lesion induces a GC to TA transversion which has been observed in the ras and p53 genes in lung and liver cancer (8) as well as skin cancers (14). This implies that ROS and RNS-mediated DNA damage may participate in carcinogenesis via activation of proto-oncogenes and inactivation of tumor suppressor genes (8). Malignant tumors often demonstrate increased levels of DNA base oxidation-induced mutations (11) as well as depleted levels of enzymes that defend against oxidative stress.

Solar UV light, particularly UVB (wavelength 280-320 nm), is recognized as being responsible for the development of skin cancers in humans and other animals (14). Therefore, the Girardi laboratory has begun investigating UVB irradiation of murine skin as a second model of carcinogenesis, complementary to the chemical model. It is not yet known if LC are needed for UVB-induced tumorogenesis as has been clearly demonstrated in chemically-induced tumor formation. However, preliminary studies in the Girardi laboratory show that following chronic UVB exposure, there are fewer p53 clonal islands, a precursor to tumor formation, in LC-deficient epidermis compared to LC-intact controls (data unpublished).

UVB exposure increases reactive oxygen species (ROS) in epidermal cells and activates signaling pathways involved in regulating cell growth, differentiation and proliferation, thus facilitating the clonal expansion of tumor cells (11). Additionally, UVB-induced production of $H_2O_2$ promotes the phosphorylation of mitogen-activated protein kinases (MAPK) such as ERK1/2 which activate growth factors and may start the process of tumorgenesis, as well as Jun NH2-terminal kinase (JNK) which may stimulate tumor inflammation, invasion, metastasis and angiogenesis (11). Furthermore, mice deficient in the repair enzyme for oxidized DNA lesions, 8-oxoguanine-DNA glycosylase, are significantly more susceptible to UVB-induced skin cancer. These mice develop both a greater number of tumors and develop tumors earlier, incriminating ROS-induced DNA mutations in carcinogenesis caused by UVB exposure (14).

Zhang *et al* have used UVB irradiation of murine skin to induce p53 clonal islands which progress to tumors. Recently, members of the Girardi lab have used this method to investigate carcinogenesis. As expected, chronic UVB exposure (12,500 $J/m^2$,

five days per week for five weeks) produced p53 mutant clonal islands within normal mouse epidermis which could be visualized by immunohistochemical staining. However, confocal examination of these epidermal sheets revealed Langerin+ MHC-II+ dendritic cells (data unpublished) which is intriguing because prior studies have reported that UVB exposure causes LC to migrate out of the epidermis and undergo apoptosis (16). This provokes the question whether these dendritic cells were LC originally located in the epidermis or if they were recruited from elsewhere such as bone marrow, dermis or peripheral blood. If recruited bone marrow-derived monocytes, they may be present in both LC-intact and transgenic LC-deficient mice. Furthermore, could this population of $Langerin^{+}$ $MHC\text{-}II^{+}$ dendritic cells, regardless of their origin, be involved in the promotion of p53 mutation, survival and proliferation of these mutated cells, potentially through increased levels of oxidative stress-induced mutations?

LC encountering stressful conditions such as endotoxin exposure, UV radiation or chemical contact, up-regulate the expression of inducible nitric oxide synthase (iNOS) which converts L-arginine into nitric oxide (NO), a RNS implicated in cellular signaling, damage, apoptosis and necrosis (12, 17). Other immune cells, such as macrophages also up-regulate iNOS expression upon activation, but whereas macrophages must first be recruited to the epidermis, LC are the major source of iNOS formed by cells that are resident in the skin (17). When exposed to the endotoxin lipopopolysaccharide (LPS), the murine LC-like cell line, XS-52, demonstrates a concentration-dependent increase in iNOS mRNA as quantified by RT-PCR in addition to bright cytoplasmic anti-iNOS immunofluorescent staining. Similarly, LPS-treated human neonatal foreskin demonstrates bright cytoplasmic anti-iNOS staining in LC (17). TNF-α (as well as IL-1-

β and INF-γ) stimulates the expression of iNOS in LC in addition to other inflammatory cells. Knockout of the TNF-α gene in mice significantly inhibits the development of skin tumors in response to DMBA and phorbol esters (12). It is unknown if a decrease in the production of iNOS and subsequent RNS in TNF-α knockout mice may be responsible for the reduction in carcinogenesis. iNOS-induced RNS production may have the paradoxical effect of potentially playing a role in immunosurveillance by inducing apoptosis or necrosis in tumor cells or, conversely, inducing mutations that accumulate to promote carcinogenesis.

It is intriguing to consider that the mechanism through which LC enhance tumorgenesis may be through effects on the level of oxidative stress in the epidermis.

**III. DNA Damage:**

Double stranded DNA (dsDNA) breaks play an important role in carcinogenesis. These DNA lesions may lead to genetic mutations and cancer or, paradoxically, may induce apoptosis of cancer cells. dsDNA breaks may be induced by irradiation, chemical agents, reactive oxygen species, recombination events during meiosis, and as a result of DNA fragmentation during apoptosis (18, 19). As cells subjected to UV irradiation and chemically-induced DNA damage enter S-phase, replication forks stall at the site of DNA lesions, which then causes activation of endonucleases that cleave the DNA, thus generating dsDNA breaks (18, 20).

Histone H2AX is one of the 5 main histone proteins involved in the structure and stability of chromatin in eukaryotic cells. In response to dsDNA breaks, histone H2AX is rapidly phosphorylated to become γH2AX. Following phosphorylation, γH2AX

accumulates at the break site, creating a focus where proteins involved in DNA repair and chromatin remodeling congregate. Following the subsequent repair and rejoining of DNA, γH2AX is unphosphorylated (19). Immunofluorecent (IF) staining using anti-γH2AX antibody reveals discrete nuclear foci at sites of dsDNA breaks. The determination of γH2AX foci provides a quantitative tool in measuring dsDNA breaks induced by DNA damaging agents (18).

The mechanism through which LC facilitate epithelial tumor development is not understood. It may be through initiation of genetic mutations through enabling increased levels of DNA damage or through increased levels of damaging oxidative stress. Investigation into this question may provide guidance for cancer prevention and immunotherapy.

## Statement of Purpose, Specific Hypothesis, and Specific Aims

The purpose of this study is to investigate how LC facilitate the development of epidermal papilloma and squamous cell carcinoma, specifically, via their potential influence on oxidative stress and DNA damage.

*Hypothesis*

1. LC facilitate development of epidermal papilloma and squamous cell carcinoma by increasing levels of oxidative stress in response to chemical or UV exposure.
2. LC facilitate development of epidermal papilloma and squamous cell carcinoma by promoting DNA damage in keratinocytes.

*Specific Aims*

1. Determine whether LC-deficient mouse epidermis has lower levels of oxidative stress compared to normal littermate controls after exposure to DMBA/TPA or UVB irradiation.
2. Determine whether LC-deficient mouse epidermis has fewer epidermal dsDNA breaks compared to normal littermate controls after exposure to DMBA/TPA or UVB irradiation.

## Methods:

Note: The author performed all procedures and data collection described in the methods section. All procedures were performed following IACUC guidelines.

*Mice*

FVB mice were obtained from Jackson Laboratory (Bar Harbor, ME).

LangDTA (Langerin diphtheria toxin A) mice on a FVB background, courtesy of the Kaplan laboratory, have a constitutive and durable absence of epidermal Langerhan cells achieved by regulatory elements from human langerin driving expression of diphtheria toxin (6).

huLangDTR (human Langerin diphtheria toxin receptor) mice on a FVB backgound, courtesy of the Kaplan laboratory, have normal populations of epidermal LC which express transgenic huLangerin. Within two days of intra-peritoneal injection with diphtheria toxin, LC undergo selective apoptosis rendering the animal completely of depleted of LC that do not begin to return for four weeks (21).

The Institutional Animal Care and Use Committee approved all mouse protocols.

*Genotyping mice*

Mice underwent a small tail biopsy (~0.5cm) for genotyping and toe clipping for identification at 10-12 days of age. PCR was used to distinguish LangDTA or huLangDTR mice from normal littermate controls. Mice for all experiments were seven weeks old and sex matched.

*Ablation of LC in huLangerin-DTR mice:*

Intra-peritoneal injection of 400ng of diphtheria toxin efficiently ablated LC in the epidermis.

*Dorsal skin depilation*

Dorsal skin of seven week old mice (at this age mouse hair is in telogen) was shaved with electric clippers then covered with depilatory cream (Nair; Church &Dwight Co., Princeton, NJ) for 3 minutes. The cream was washed off with water and Vasaline was applied to the area. Skin was allowed one week to recover before UVB or chemical treatment

*UVB Irradiation:*

Mice are anesthetized with Avertin, laid prone and put into a UVB chamber. For experiments where ears are investigated, they were taped horizontal to the UVB bulbs for even exposure. The UVB irradiation chamber contains a bank of four UVB lamps (FS20T12-UVB; National Biological Corp., Twinsburg, OH) that emit 250-420nm (72.6% UVB; 27.4% UVA; 0.01% UVC), peak 313nm. A filter (Kodecel TA422; Eastman Kodak, Rochester, NY) was used to block residual UVC. Dosimetry was determined by a calibrated UVB-500C meter (National Biologic Corp.).

*Chemical treatment*

Dorsal skin was treated with 200nmol or 400nmol of 7,12-

dimethylbenz[a]anthracene (DMBA) in acetone or 5nmoles or 20nmoles of 12-O-tetradecanoylphorbal-13-acetate (TPA) in 100% ethanol.

*Epidermal sheet preparation*

Animals were euthanized by Avertin anesthesia. Death point determined by absence of cardio-vascular function was followed by cervical dislocation. Treated skin was excised from the back (3cm x 1.5cm) or the ears were cut off. Subcuticular fat was scraped from the dermis. Sheets of skin were placed epidermal-side-up in a petri dish containing 20mM EDTA in PBS, pH 7.4 and incubated at 37°C for 2 hours. The epidermis was then separated from the dermis and washed in PBS. The epidermal sheets were then laid flat and fixed in cold (on ice) acetone for 20 minutes then washed again in PBS.

*Immunofluorecent staining for 8oxoG*

Epidermal sheets were blocked in 2% BSA in PBS and 10% Donkey and/or Goat serum for one hour at 37°C. This was followed by incubation in the primary antibody at 4°C or 37°C for 90 minutes. Primary antibodies used were: rat anti-mouse CD207 (Langerin) (eBioscience 14-2073); mouse anti-8-oxoguanine, clone 483.15 (Millipore MAB3560); anti-pan cytokeratin FITC conjugate, clone C-11 (Sigma F3418); FITC anti-mouse γδTcell receptor (GL3) (BD Pharmingen 553177); Cy3 conjugated Goat Anti-mouse IgM (isotype-matched control for 8oxoG) (Jackson 115-166-020). Sheets were then washed in PBS and incubated in the secondary antibody at 37°C for 90 minutes. Secondary antibodies used were: goat anti-mouse Cy3 (Jackson 115-166-020); donkey

anti-rat Cy5 (Jackson 712-175-153). Finally, the sheets were washed once more in PBS.

*Immunofluorescent staining for γH2AX*

Epidermal sheets were permeabilized in 0.5% Triton and 0.5% BSA in PBS for 30 minutes at room temperature (RT). Then they were then blocked in 1:1000 Donkey IgG in 0.5% Triton PBS/BSA (0.5%) for 30 minutes at RT followed by incubation in primary antibody at 4°C overnight: Abcam Rabbit polyclonal to gamma H2A.X (phospho S139)-DNA double-strand break marker (ab2893) 1:400 in permeabilization solution. Epidermal sheets were washed in permeabilization solution and incubated in secondary antibody for one hour at RT: FITC conjugated AffiniPure Doney Anti-Rabbit IgG (H+L) (Jackson 711-095-152) at 1:200 in 0.5% Triton PBS/BSA (0.5%).

*Mounting epidermal sheets on slides*

Fixed, stained epidermal sheets were positioned flat on slides, basal side down. One drop of ProLong Gold antifade reagent (Invitrogen) was placed over each sheet. A coverslip was applied and sealed with clear nail varnish (Sally Hanson). Slides were blinded by randomly assigning a number to each slide. Results were quantified on a Zeiss Meta 510 confocal microscope. Slides were then unblinded and results were assessed using ImageJ software (NIH).

*Statistical Analysis*

Prism software (Graphpad, San Diego, CA) was used to analyze data with an ANOVA or two-tailed t-test. A p-value ≥0.05 was considered significant.

## Results

### I. Oxidative Stress in UVB-induced Carcinogenesis

Immunofluorescent (IF) staining of the epidermis with 8oxoG demonstrated oxidative stress in all cell types, including keratinocytes, T-cells, and LC. The punctate cytoplasmic pattern observed suggests ribosomal staining, which would be consistent with specific staining for oxidized guanine (Figure 1). The epidermal sheets were not treated to permeabilize the nucleus because this would have required treatment with either an acid or base, both of which would have increased levels of background oxidative stress. The dose of UVB irradiation, 33600J/$m^2$, is a higher dose than used by Zhang, *et al.* However, a high dose may allow us to see more subtle differences between LC-intact and LC-deficient mice and to better overcome background oxidative stress produced by processing epidermal sheets.

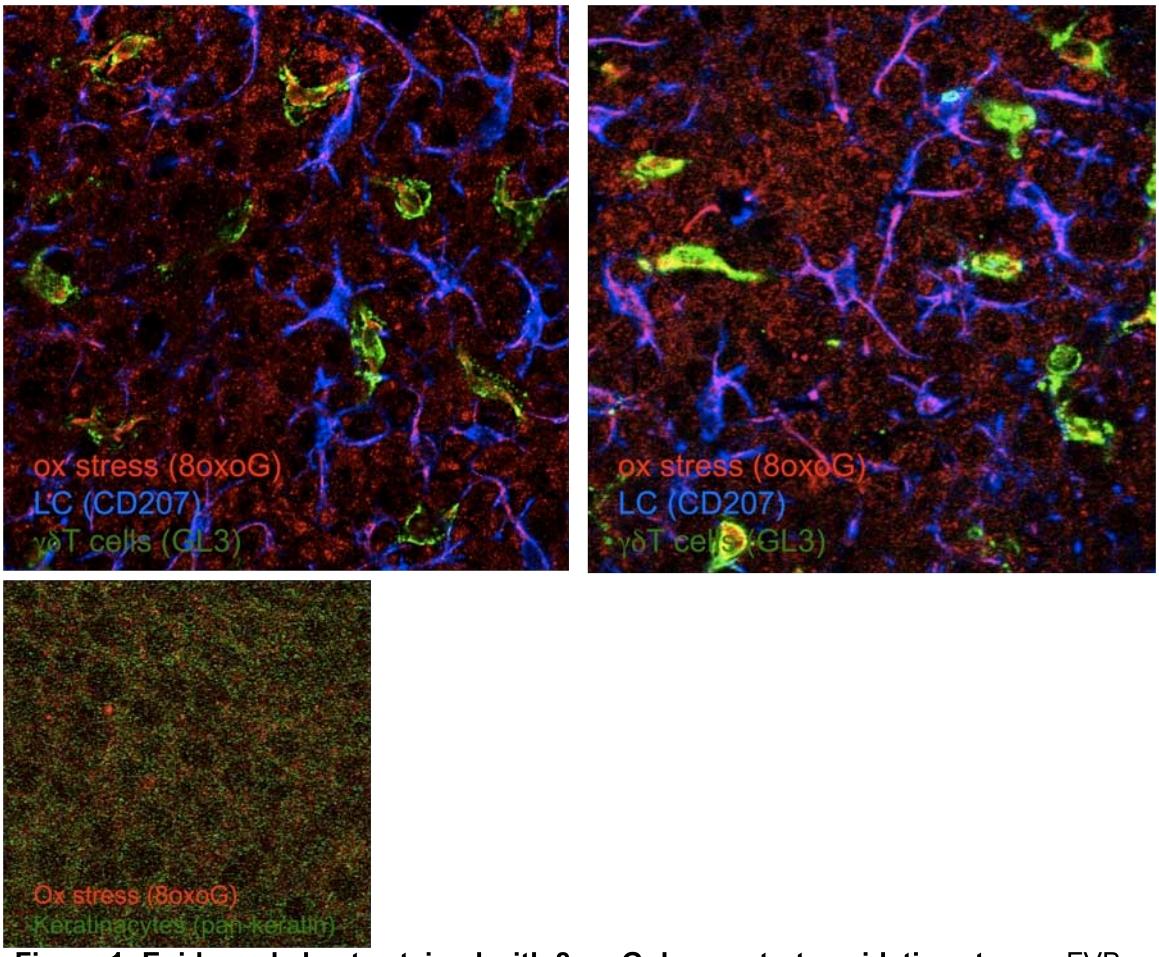


**Figure 1: Epidermal sheets stained with 8oxoG demonstrate oxidative stress.** FVB dorsal epidermis was exposed to 33600J/m$^2$ of UVB irradiation and skin was harvested immediately. Keratinocytes, LC, and T-cells all stain 8oxoG$^+$, indicating they are susceptible to UVB-induced oxidative stress.

In order to assess the feasibility of using 8oxoG IF to quantify UVB-induced levels of oxidative stress, FVB murine dorsal skin was depilated and exposed to 0 J/m$^2$, 8400 J/m$^2$, or 33600 J/m$^2$ of UVB irradiation. Oxidative stress was assessed by the overall intensity of staining in the 8oxoG channel in each high power field (hpf) measured in relative intensity units (RIU). The intensity of 8oxoG staining increased with rising levels of UVB exposure: the mean 8oxoG following 0 J/m$^2$ UVB was 100.0±12.5 RIU, after 8400 J/m$^2$ it rose to 113.8±12.0 RIU, and 142.9±15.3 RIU

subsequent to 33600 J/$m^2$. Although the difference was not statistically significant using a 1 way ANOVA test, the trend was clear. Many different types of epidermal cells, including keratinocytes and dendritic, cells were 8oxoG$^+$, suggesting that many, if not all, epidermal cell types are susceptible to UVB-induced oxidative stress. Hair follicles and folds/irregularities in the epidermis may have negatively affected the accuracy of measurements and the number of mice was small (n=5), however, a large number of random 25x fields were assessed to overcome these confounding factors (Figure 2).

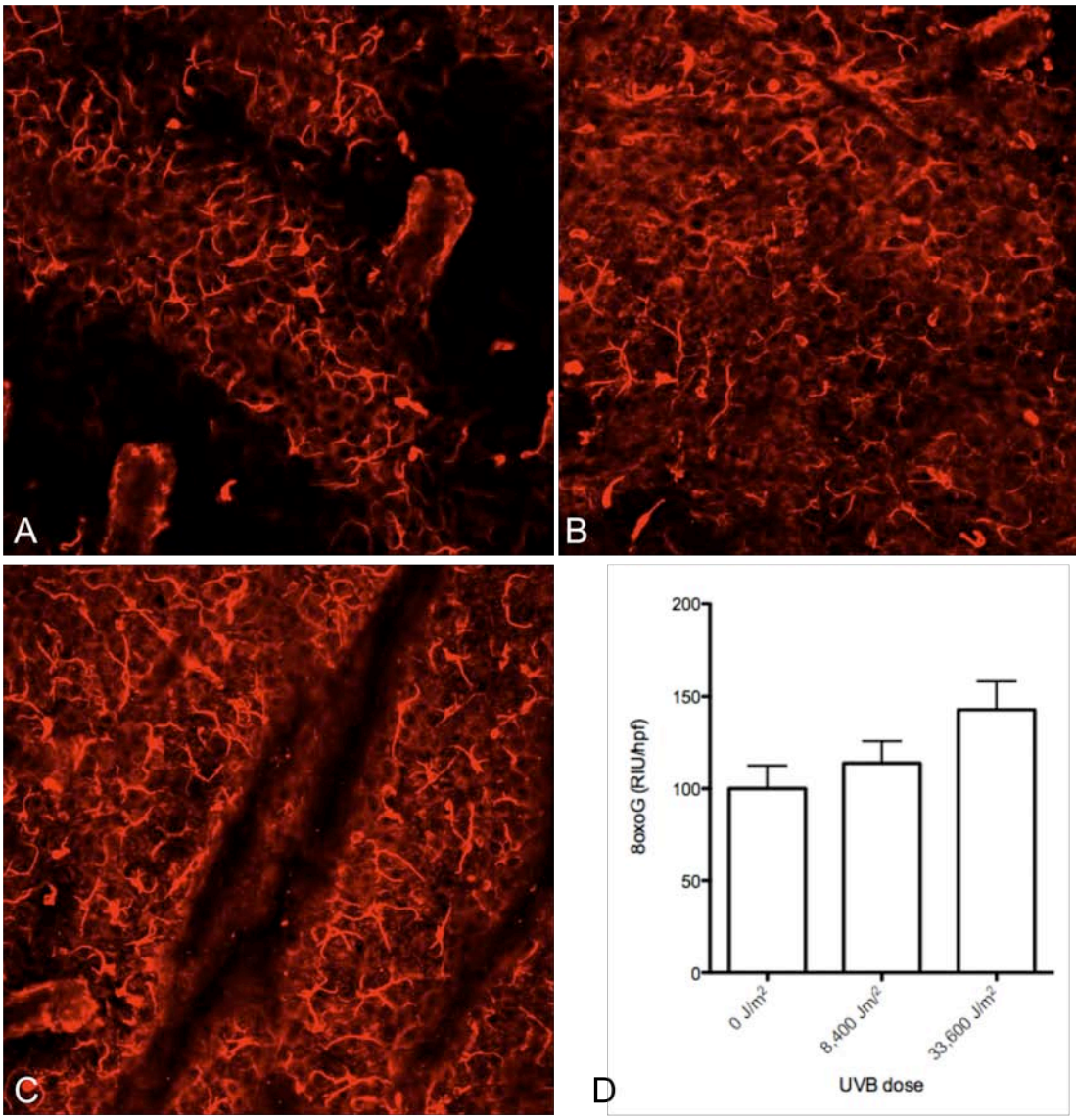


**Figure 2: 8oxoG IF staining indicates increased levels of oxidative stress with increasing dose of UVB.** FVB murine dorsal epidermis exposed to UVB irradiation and stained immediately for oxidative stress (red; 8oxoG) **(A)** 0 J/m$^2$ **(B)** 8400 J/m$^2$ **(C)** 33600 J/m$^2$ **(D)** Increasing intensity of 8oxoG with increasing levels of UVB exposure.

Ear epidermis, unlike dorsal skin, does not require chemical depilatory cream and shaving for hair removal before UVB treatment. This may make ear skin more desirable than dorsal skin for oxidative stress experiments as depilatory cream and shaving may increase levels of background oxidative stress and inflammation and may lead to uneven hair removal and therefore uneven exposure to UVB. Ears, however, are subject to

continual small traumas due to their position on the side of the head. To determine the potential usefulness of ears in the assessment of UVB-induced epidermal oxidative stress, FVB mouse ears were exposed to either 0 $J/m^2$ or 33600 $J/m^2$ of UVB irradiation (n=12 ears). Ears were taped so that they were positioned horizontal to the UVB bulbs in order to obtain an even dose of irradiation. Ten high power fields (hpf) at 25x, 3mm apart were quantified per ear. The mean intensity of 8oxoG staining in the non-irradiated ears was 100.0±11.7 RIU whereas the mean in the 33600 $J/m^2$ group was significantly higher at 155.0±14.6 RIU, p=0.002 (Figure 3).

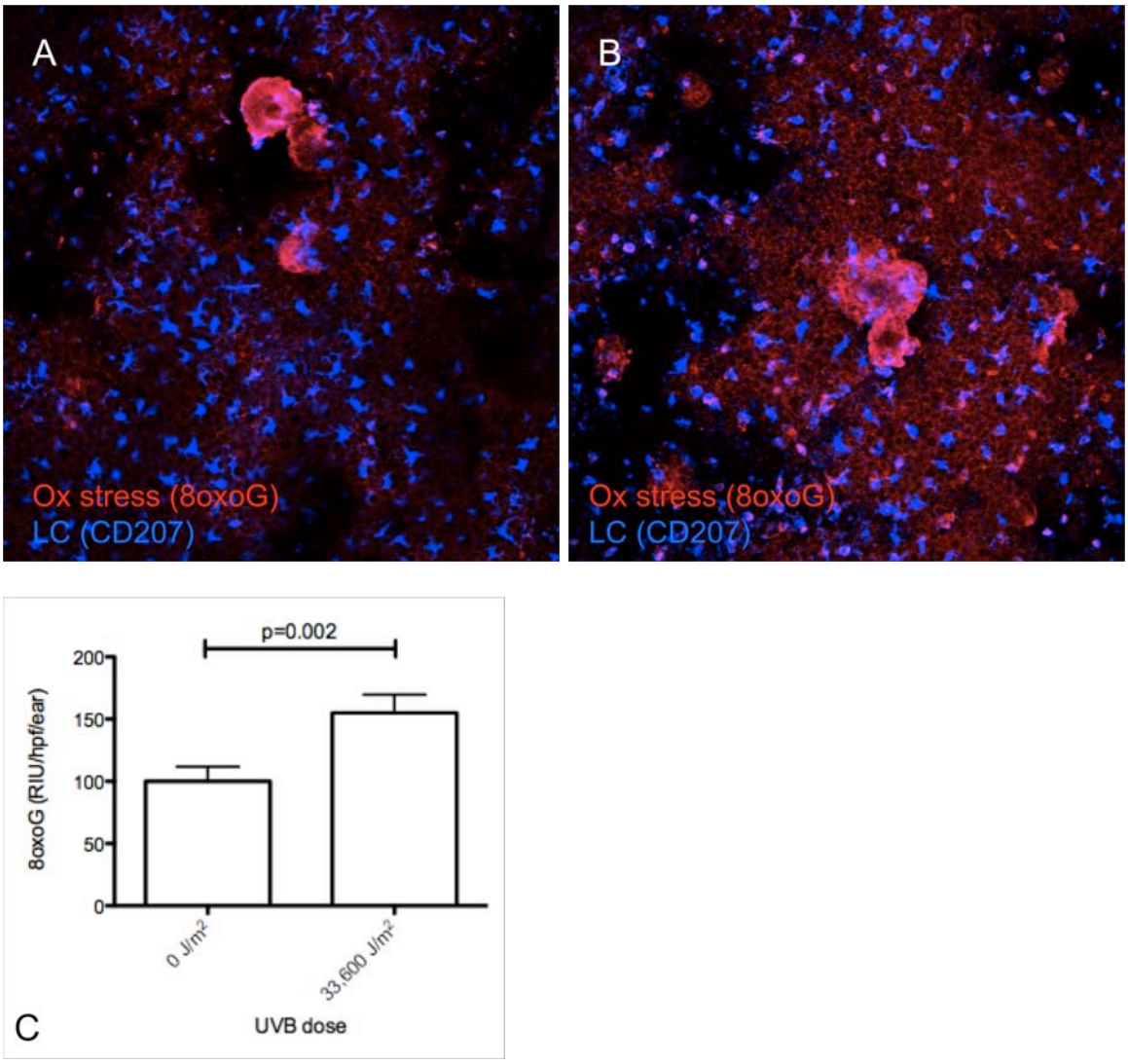


**Figure 3. 8oxoG IF staining indicates increased levels of oxidative stress following UVB irradiation.** FVB murine ear epidermis exposed to UVB irradiation and stained immediately showed an increase in 8oxoG RIU following 33600J/m$^2$ of UVB irradiation compared to non-irradiated controls. (**A)** 0 J/m$^2$ (**B)** 33600 J/m$^2$ **(C)** significant increase in 8oxoG intensity per hpf per ear following UVB exposure

In order to better understand the role of LC in oxidative stress, LC-deficient and LC-intact normal littermate control (NLC) mouse ears were exposed to 33600J/m$^2$ of UVB irradiation (n=12 ears). Oxidative stress levels as quantified using 8oxoG were higher in the LC-deficient epidermis with a mean of 96.3±27.6 RIU in NLC and 179.2±13.6 RIU in LangDTA epidermis, p=1.04x10$^{-4}$ (Figure 4). To negate the potential

confounding affect of oxidative stress within LC rather than keratinocytes, the LC were subtracted from the images of FVB epidermis before 8oxoG levels were quantified (Figure 4b).

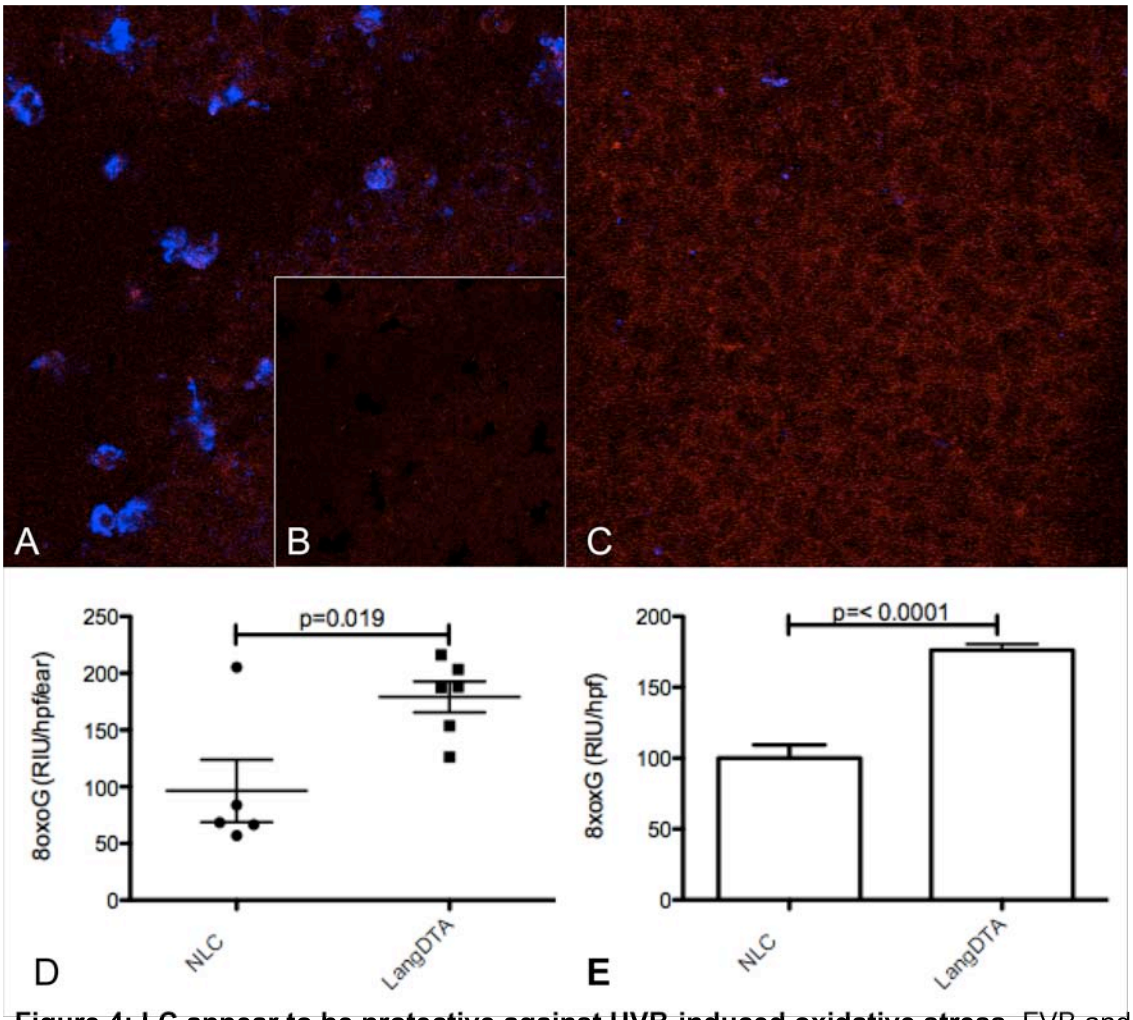


**Figure 4: LC appear to be protective against UVB-induced oxidative stress**. FVB and LangDTA mouse ears were exposed to 33600J/m$^2$ of UVB irradiation, harvested immediately and stained for oxidative stress (red; 8oxoG) and LC (blue; CD207) **(A)** FVB epidermis **(B)** FVB epidermis with LC subtracted **(C)** LangDTA epidermis **(D)** Analysis by ear **(E)** Analysis by hpf

T-cells may have an effect on how LC function, therefore we were interested in

investigating whether the effect of LC on oxidative stress is influenced by the presence of T-cells. T-cell deficient ($\beta^{-/-}\delta^{-/-}$) mice were used to determine the potential role of T-cells. $\beta^{-/-}\delta^{-/-}$FVB and $\beta^{-/-}\delta^{-/-}$LangDTA mice were exposed to 33600 J/m$^2$ of UVB irradiation and the levels of 8oxoG were assessed. The results were consistent with the previous experiment; LC-deficient epidermis had higher levels of oxidative stress compared to FVB controls, 965.7±186.8 RUI and 453.4±76.0 RIU respectively, p=0.029 (Figure 5).

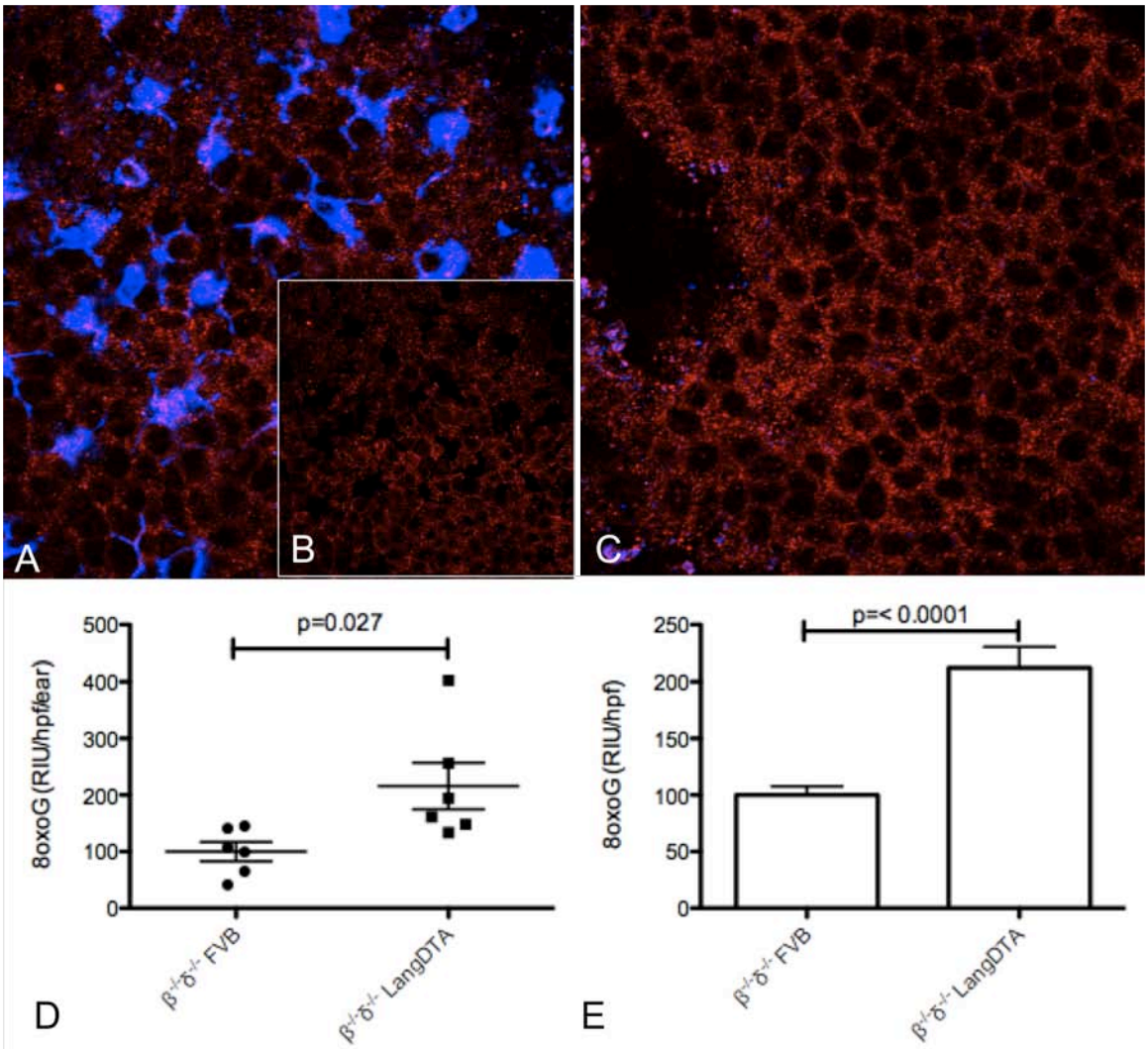


**Figure 5: LC appear to be protective against UVB-induced oxidative stress independent of T-cells.** $\beta^{-/-}\delta^{-/-}$ FVB and $\beta^{-/-}\delta^{-/-}$ LangDTA mouse ears were exposed to 33600J/$m^2$ of UVB irradiation, harvested immediately and stained for oxidative stress (red; 8oxoG) and LC (blue; CD207) **(A)** $\beta^{-/-}\delta^{-/-}$ FVB epidermis **(B)** $\beta^{-/-}\delta^{-/-}$ FVB epidermis with LC subtracted **(C)** $\beta^{-/-}\delta^{-/-}$ LangDTA epidermis **(D)** Analysis by ear **(E)** Analysis by hpf

We attempted to find a method of epidermal fixation that would produce a lower level of background oxidative stress. However, all alternative methods had substantial drawbacks.

Frozen sections allow the epidermis to be stained with IF while producing

minimal background oxidative stress. In contrast, separating the epidermis from the dermis to produce epidermal sheets requires the use of oxidative stress-inducing chemicals. Unfortunately, frozen sections produce nonspecific keratin staining, provide a very small area of epidermis for quantification per image and introduce the additional confounding factor of the angle of cut relative to the epidermis (Figure 6).

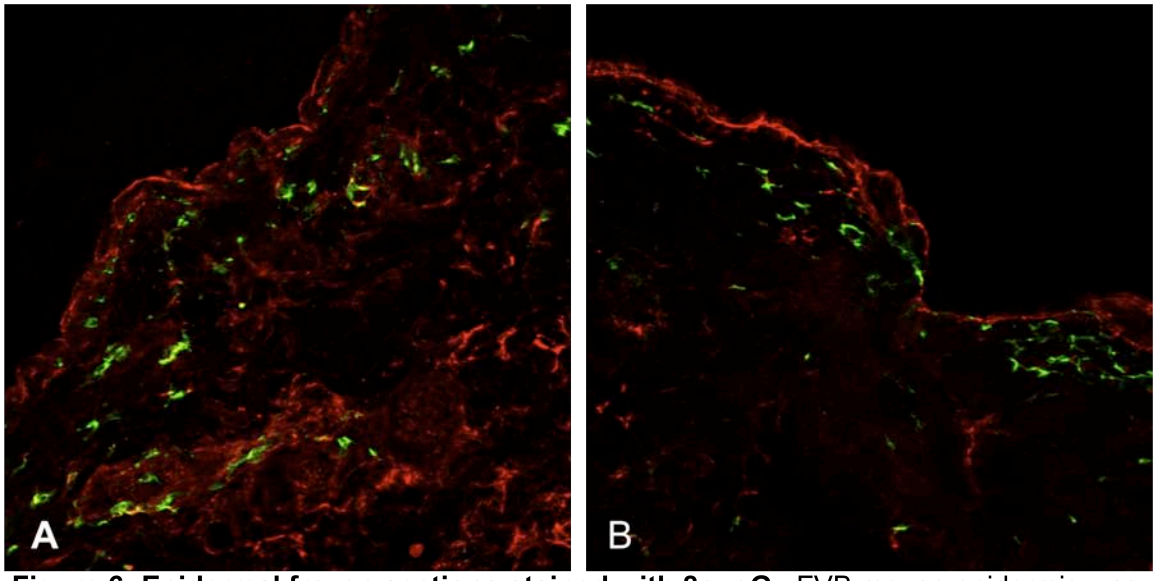


**Figure 6: Epidermal frozen sections stained with 8oxoG.** FVB mouse epidermis was exposed to 0 J/m$^2$ or 33600 J/m$^2$ of UVB irradiation, harvested immediately and stained for oxidative stress (red; 8oxoG) and LC (green; MHCII). The epidermal area available for quantifying results is small and largely dependent on the angle of the cut relative to the epidermis, and there is nonspecific keratin staining. **(A)** 0 J/m$^2$ UVB irradiation, cut not exactly perpendicular to the epidermis **(B)** 33600J/m$^2$ UVB irradiation, cut perpendicular to the epidermis

LC are known to migrate out of the epidermis and apoptose following UVB irradiation (11), therefore we were interested in whether LC may be more susceptible to oxidative stress than other epidermal cells. To investigate this, the number of LC per hpf were counted in FVB mouse un-irradiated ear epidermis and epidermis irradiated with 33600 J/m$^2$. The mean number of LC after 0 J/m$^2$ was 126.4 ±7.0 compared to 105.0

±6.3 in ears exposed to 33600 J/m$^2$ UVB irradiation, p=0.017. This is a significant decrease, however, it is anticipated that if the skin had not been harvested immediately following irradiation, but a few days later, the number of LC present in the epidermis may have continued to decrease. The percent of remaining LC that displayed oxidative stress was not significantly different between groups, with 19.85±2.1 after 0 J/m$^2$ and 18.1±2.0 following 33600 J/m$^2$, p=0.27 (Figure 7). It is reasonable to consider that many of the most stressed LC may have migrated out of the epidermis or undergone apoptosis.

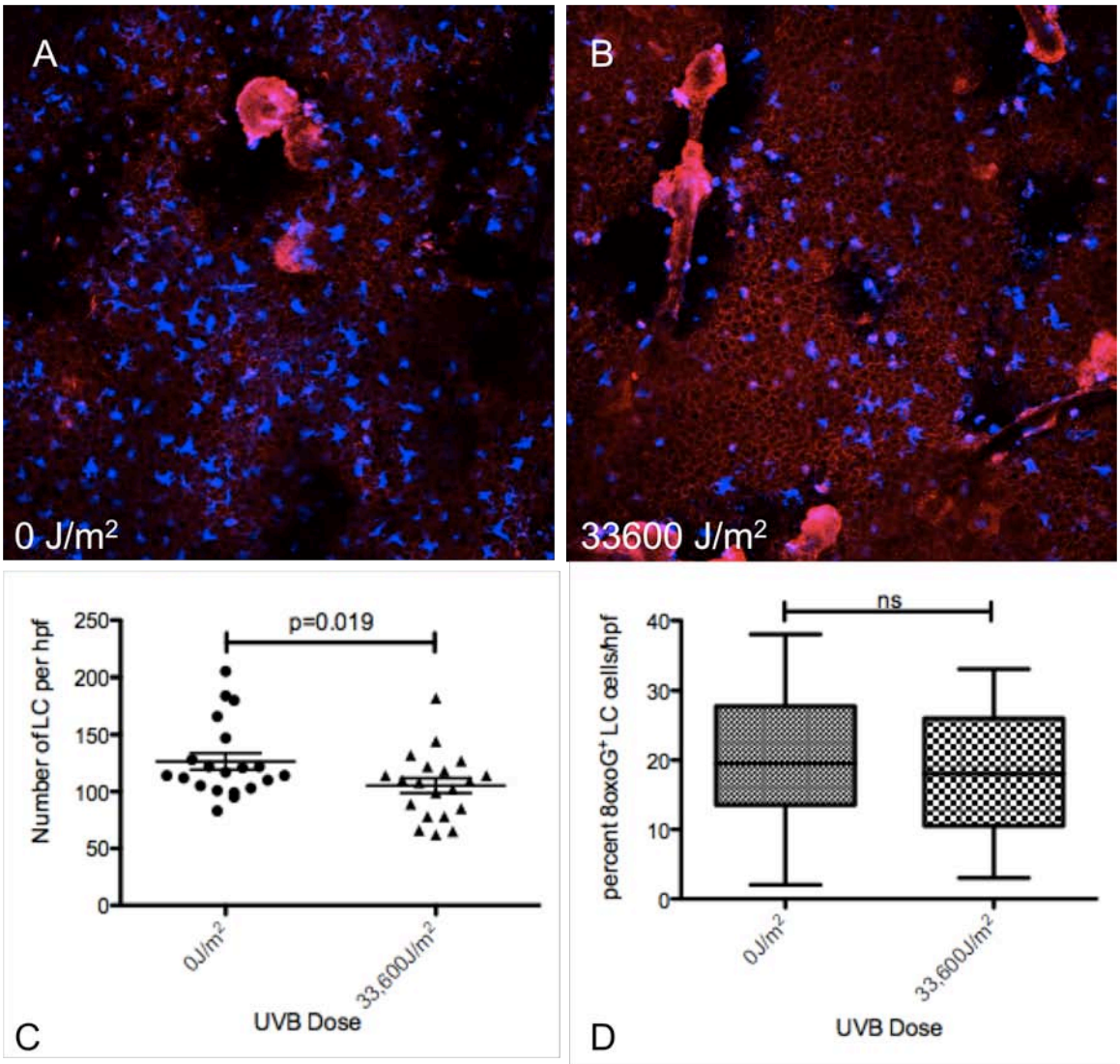


**Figure 7: The number of LC per hpf decreases following UVB irradiation, however the percent of remaining LC that are 8oxoG⁺ is unchanged.** FVB mouse ears were exposed to 0J/m$^2$ or 33600J/m$^2$ of UVB irradiation, harvested immediately and stained for oxidative stress (red; 8oxoG) and LC (blue; CD207). **(A)** FVB epidermis not exposed to UVB **(B)** FVB epidermis exposed to 33600J/m$^2$ UVB **(C)** The number of LC remaining in the epidermis decreases immediately following UVB irradiation **(D)** The percent of 8oxoG⁺ LC remaining in the epidermis is unchanged following UVB irradiation

The role of T-cells in LC migration is not understood, therefore we repeated this experiment in T-cell deficient mice. $\beta^{-/-}\delta^{-/-}$FVB ear epidermis exposed to 33600 J/m$^2$ was compared to non-exposed controls. Epidermis that was exposed to 33600 J/m$^2$ had fewer LC (88.3 ±4.25 per hpf) compared to unexposed epidermis (103.9 ±5.4 LC per hpf),

p=0.015. However, the mean percent of LC present that demonstrated oxidative stress was not significantly different. The mean percent of 8oxoG$^+$ LC after 0 J/m$^2$ was 19.2 ±2.8 and following 33600 J/m$^2$ was 25.4±2.0, p=0.05. Therefore, UVB exposure, independent of T-cells, decreases the number of LC in the epidermis compared to unexposed controls, however the percent of remaining LC that are 8oxoG$^+$ remains unchanged (Figure 8).

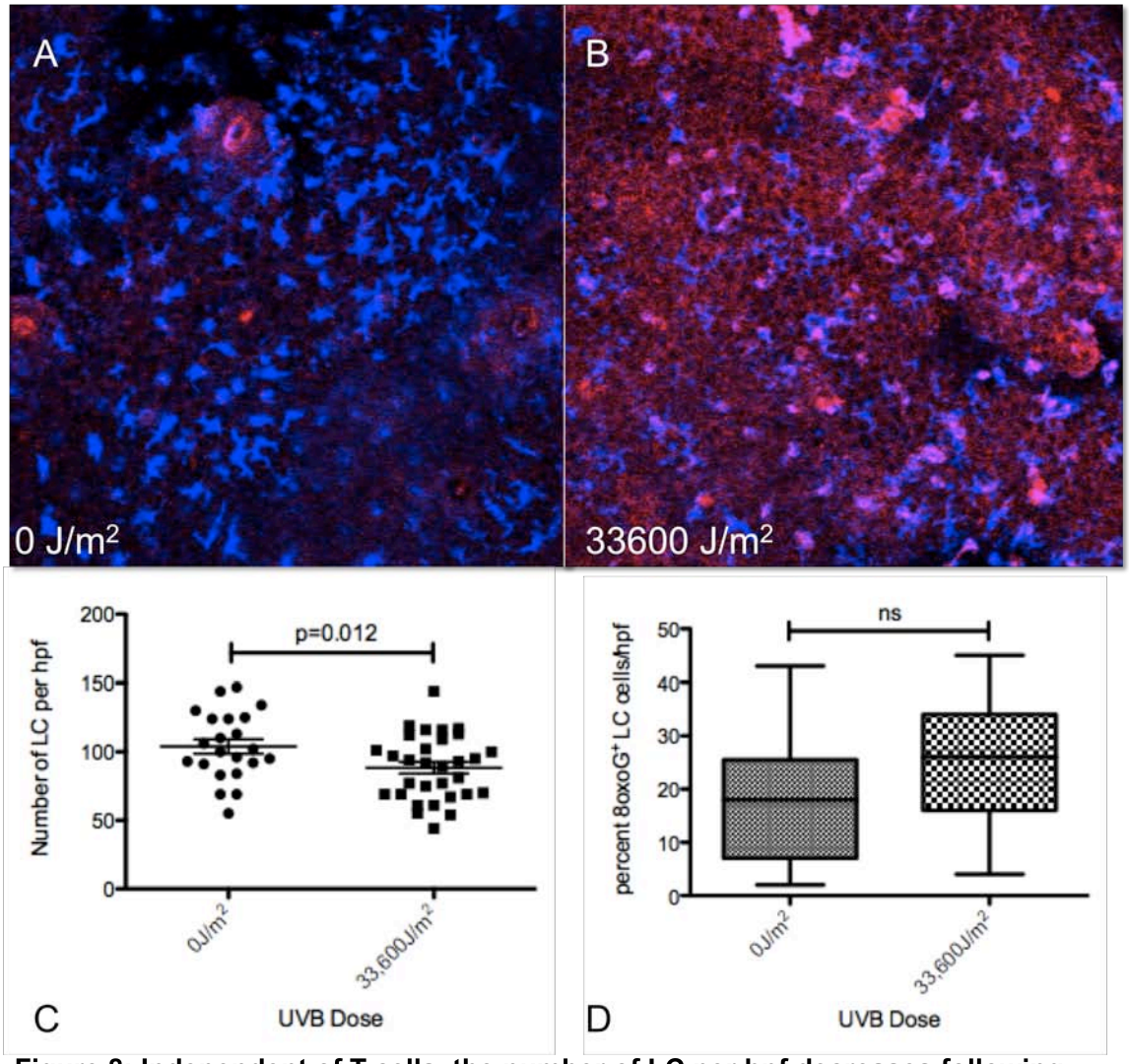


**Figure 8: Independent of T-cells, the number of LC per hpf decreases following UVB irradiation, however the percent of remaining LC that are 8oxoG$^+$ is unchanged.** $\beta^{-/-}\delta^{-/-}$FVB mouse ears were exposed to 0J/m$^2$ or 33600J/m$^2$ of UVB irradiation, harvested immediately and stained for oxidative stress (red; 8oxoG) and LC (blue; CD207). **(A)** $\beta^{-/-}\delta^{-/-}$FVB epidermis not exposed to UVB **(B)** $\beta^{-/-}\delta^{-/-}$FVB epidermis exposed to 33600J/m$^2$ UVB **(C)** The number of LC remaining in the epidermis decreases immediately following UVB irradiation **(D)** The percent of 8oxoG$^+$ LC remaining in the epidermis is unchanged following UVB irradiation

## II. Oxidative Stress in Chemically-induced Carcinogenesis

The feasibility of quantification of chemically-induced oxidative stress using 8oxoG was assessed by exposing FVB mice to 5nmol TPA and comparing the results to unexposed controls (n=16 ears). Skin was harvested four hours after TPA application.

Images were taken with the confocal microscope at 25x. Ten fields, 3mm apart were quantified per ear. The mean 8oxoG intensity in the control group was 853.1±113.6 RIU compared to 880.1±60.85 RIU in the TPA exposed group, p=0.42 (Figure 9).

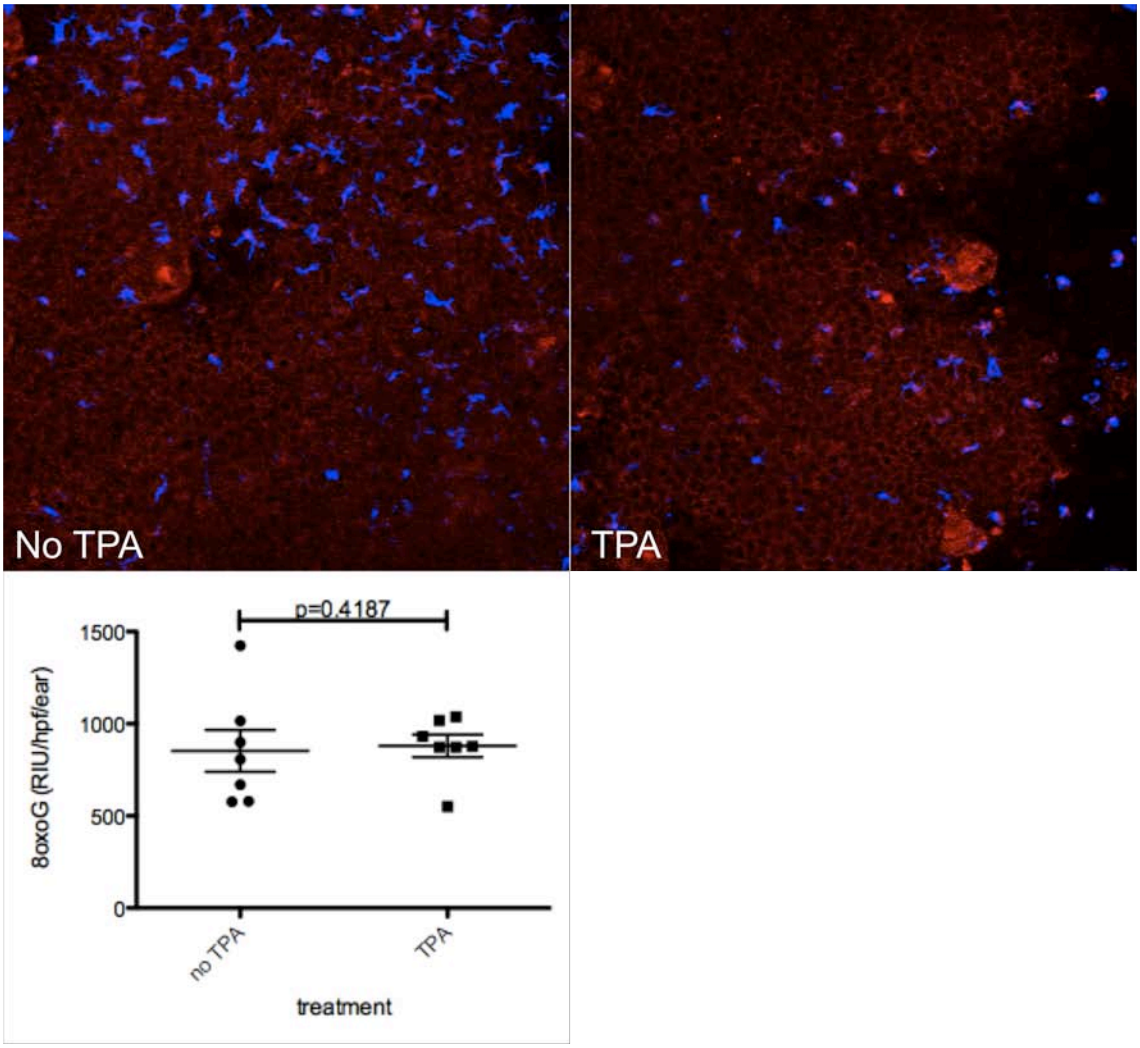


**Figure 9: No significant difference in epidermal sheet 8oxoG staining after TPA exposure.** FVB mouse ear epidermis was exposed to 5 nmol of TPA, skin was harvested four hours after treatment and epidermal sheets were stained for oxidative stress (red; 8oxoG) and LC (blue; CD207). No statistically significant difference was quantified between treated and untreated epidermis.

TPA is an inflammatory chemical; therefore we expected an increase in oxidative

stress following its application, however, our results did not support this supposition. We hypothesized that TPA may not cause significant increases in oxidative stress until neutrophils are recruited to the epidermis. Therefore, harvesting the epidermis four hours after TPA treatment may have been too soon. Furthermore, the dose of TPA may have been too low to appreciate a difference. To address these factors, we repeated this experiment using dorsal skin of FVB mice exposed to a higher dose (20nmol) of TPA applied two times with 24 hours between applications, n=13. Mice were sacrificed one hour after the second application of TPA and the epidermis was stained for 8oxoG and LC. Surprisingly, there was no statistically significant difference quantified between the TPA treated (mean 637.4±120) and untreated controls (mean 562.6±56), $p>0.05$ (Figure 10A,B). These results suggest that 8oxoG staining is not a good method of quantifying TPA-induced oxidative stress in this model.

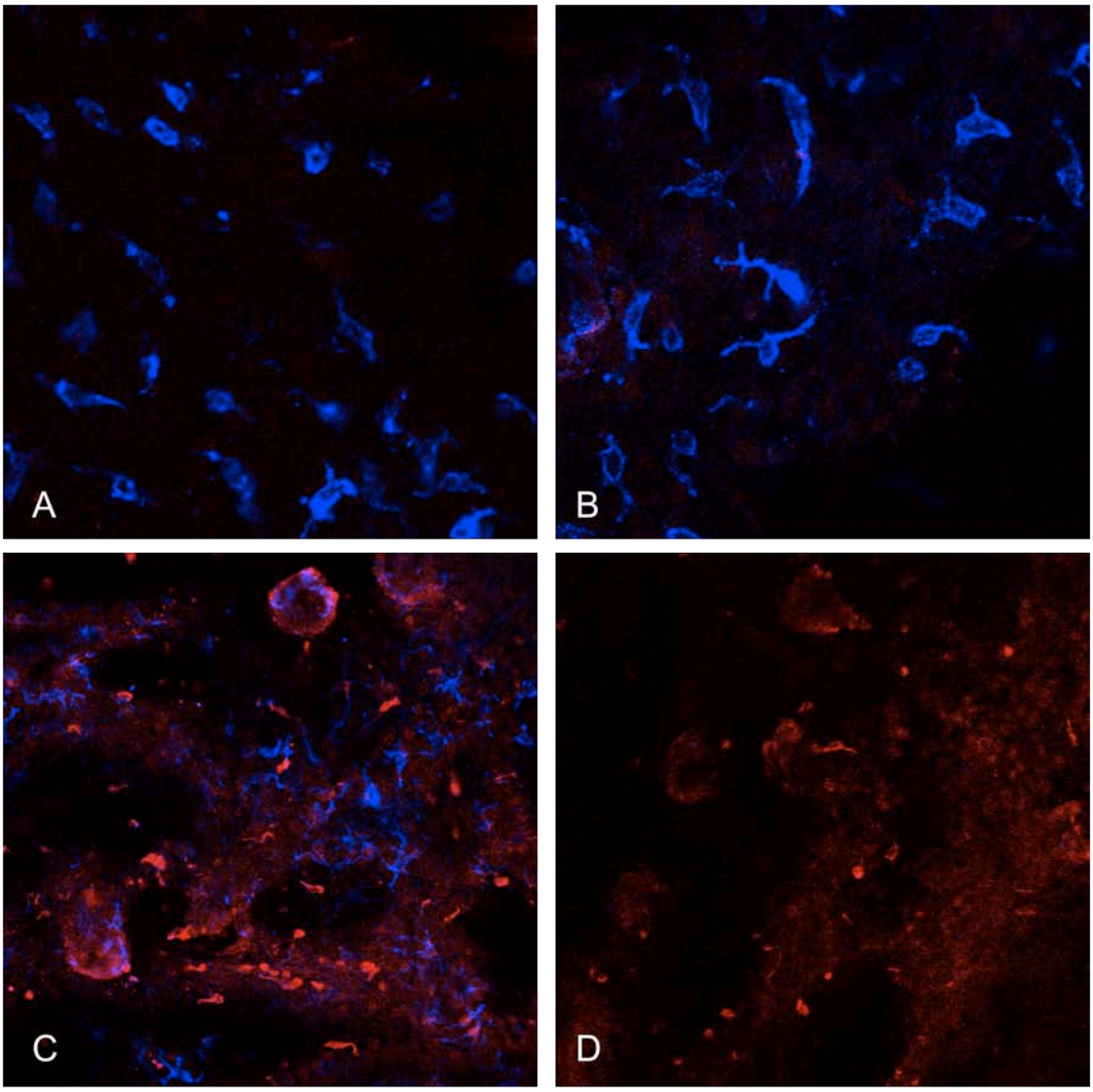


**Figure 10A: Epidermal sheets exposed to two doses of TPA.** FVB mouse dorsal epidermis was painted with 20 nmol of TPA twice, 24 hours apart, skin was harvested one hour after the second treatment and epidermal sheets were stained for oxidative stress (red; 8oxoG) and LC (blue; CD207).
**(A,B)** Confocal microscope focus on plane with LC; A. no TPA; B. TPA
**(C,D)** Confocal microscope focus on plane with keratinocytes; C. no TPA; D. TPA

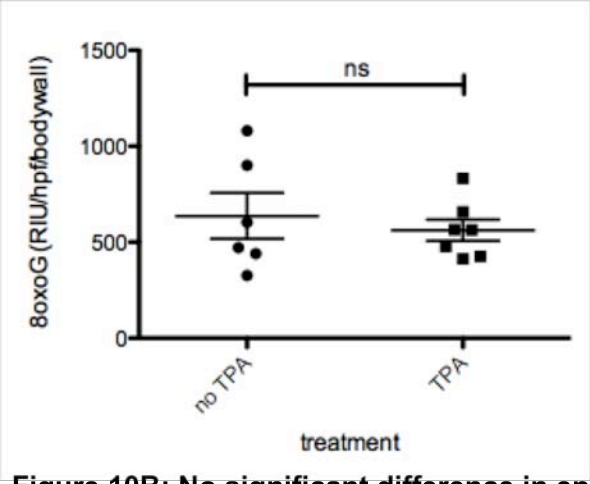


**Figure 10B: No significant difference in epidermal sheet 8oxoG staining after two doses of TPA.** FVB mouse dorsal epidermis was painted with 20 nmol of TPA twice, 24 hours apart, skin was harvested one hour after the second treatment and epidermal sheets were assessed for 8oxoG intensity. There was no significant difference between treated and untreated epidermis.

**III. Double-stranded DNA breaks in UVB-induced Carcinogenesis**

Double-stranded DNA (dsDNA) breaks can be visualized by γH2AX immunofluorescent staining. H2AX is a histone that becomes phosphorylated at sites of dsDNA damage to become γH2AX. Inaccurate repair of dsDNA breaks may be responsible for mutations that transform cells and lead to cancer. It is unknown how LC influence keratinocyte dsDNA damage.

LC-intact murine dorsal epidermis was irradiated with 67200 J/m$^2$ and compared to untreated controls to determine whether UVB-induced dsDNA breaks could be assessed by γH2AX staining. There was a statistically significant increase in γH2AX$^+$ nuclei following UVB irradiation with an increase in the average number per hpf per mouse bodywall from 3.40±0.4 to 8.34±2.4, p=0.05 (Figure 11).

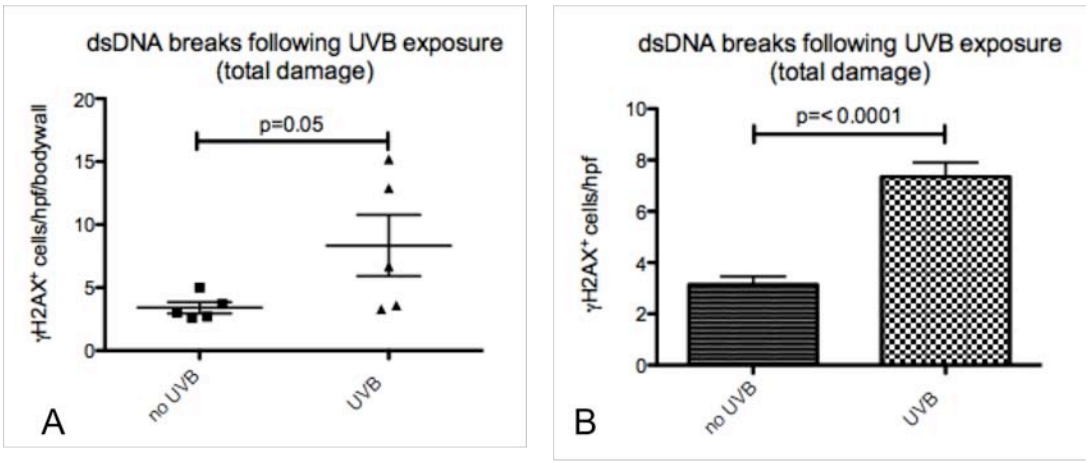


**Figure 11: γH2AX IF staining indicates increased levels of dsDNA breaks following UVB irradiation.** FVB murine dorsal skin was exposed to 67200 J/m$^2$, harvested immediately, and stained with γH2AX. **(A)** results per hpf per mouse (**B)** results per hpf

We were confident from the results of this experiment that γH2AX could be used to quantify UVB-induced dsDNA breaks. Therefore, we proceeded to investigate the role LC may play in epidermal DNA damage. LangDTA and NLC murine ears (n=24) were exposed to 67200 J/m$^2$ of UVB irradiation, harvested immediately and stained for γH2AX. Due to UVB damage, only 14 ears could be used (8 LangDTA and 6 NLC). γH2AX$^+$ nuclei were counted in 20 consecutive 63x fields per ear. There was a statistically significant increase in the number of dsDNA breaks in the LangDTA (mean 40.86±3.6) compared to the NLC (mean 25.00±2.2) epidermis, p=0.005 (Figure 12). The increase in dsDNA breaks in the LC-deficient skin suggests that LC may play a protective role against UVB-induced DNA damage.

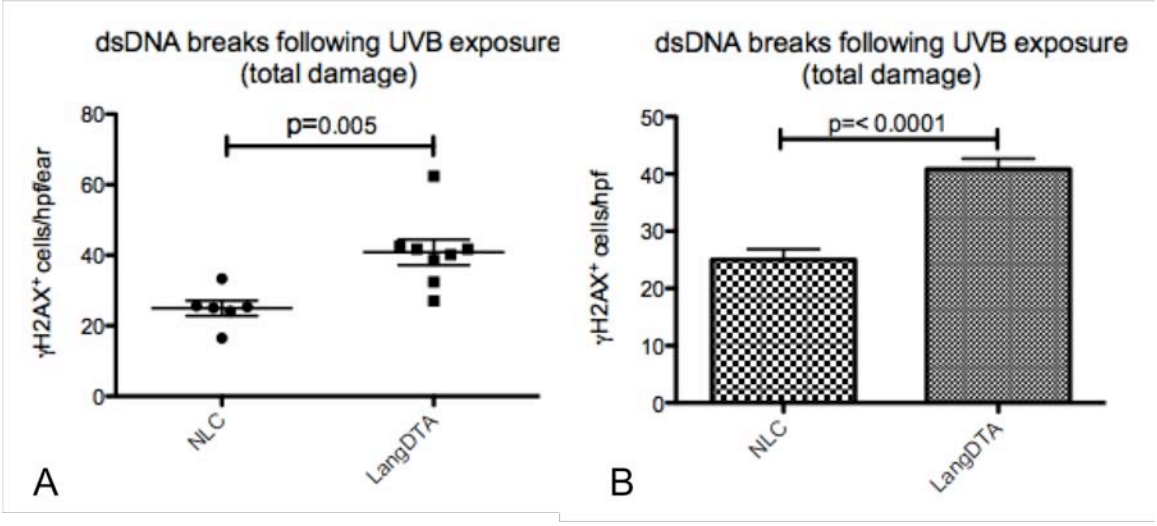


**Figure 12: LC appear to be protective against UVB-induced dsDNA breaks.** LangDTA and NLC ear epidermis was exposed to 67200 J/m$^2$ UVB irradation, harvested immediately, and stained with γH2AX. **(A)** results per hpf per ear **(B)** results per hpf

We wanted to confirm that LC are protective against UVB-induced dsDNA breaks, therefore we repeated the previous experiment with two modifications. Firstly, to reduce the physical epidermal damage, we decreased the UVB dose from 67200 J/m$^2$ to 50400J/m$^2$ and used dorsal skin rather than ears because this skin is more durable (n=8). Secondly, γH2AX$^+$ nuclei were categorized as severely damaged (the nucleus was full of γH2AX staining), intermediate damage (there were greater than five γH2AX$^+$ punctum in the nucleus), or mild damage (there were five or fewer γH2AX$^+$ punctum in the nucleus). Forty-five consecutive 63x fields were assessed in each epidermal sheet. There was no statistically significant difference between NLC (mean 14.68±1.0) and LangDTA (mean 18.55±5.8), p=0.54 epidermis in the total number of γH2AX$^+$ nuclei per hpf per mouse bodywall (Figure 13A). However, there was a significant increase in the total number of γH2AX$^+$ nuclei in LC-deficient epidermis when the results were analyzed per hpf, with 14.69±0.5 γH2AX$^+$ nuclei per hpf in NLC epidermis compared to 18.54±1.4 in

LangDTA, p=0.008 (Figure 13B). This is due to the higher *n* used when analyzing data by hpf rather than the average per hpf per mouse bodywall.

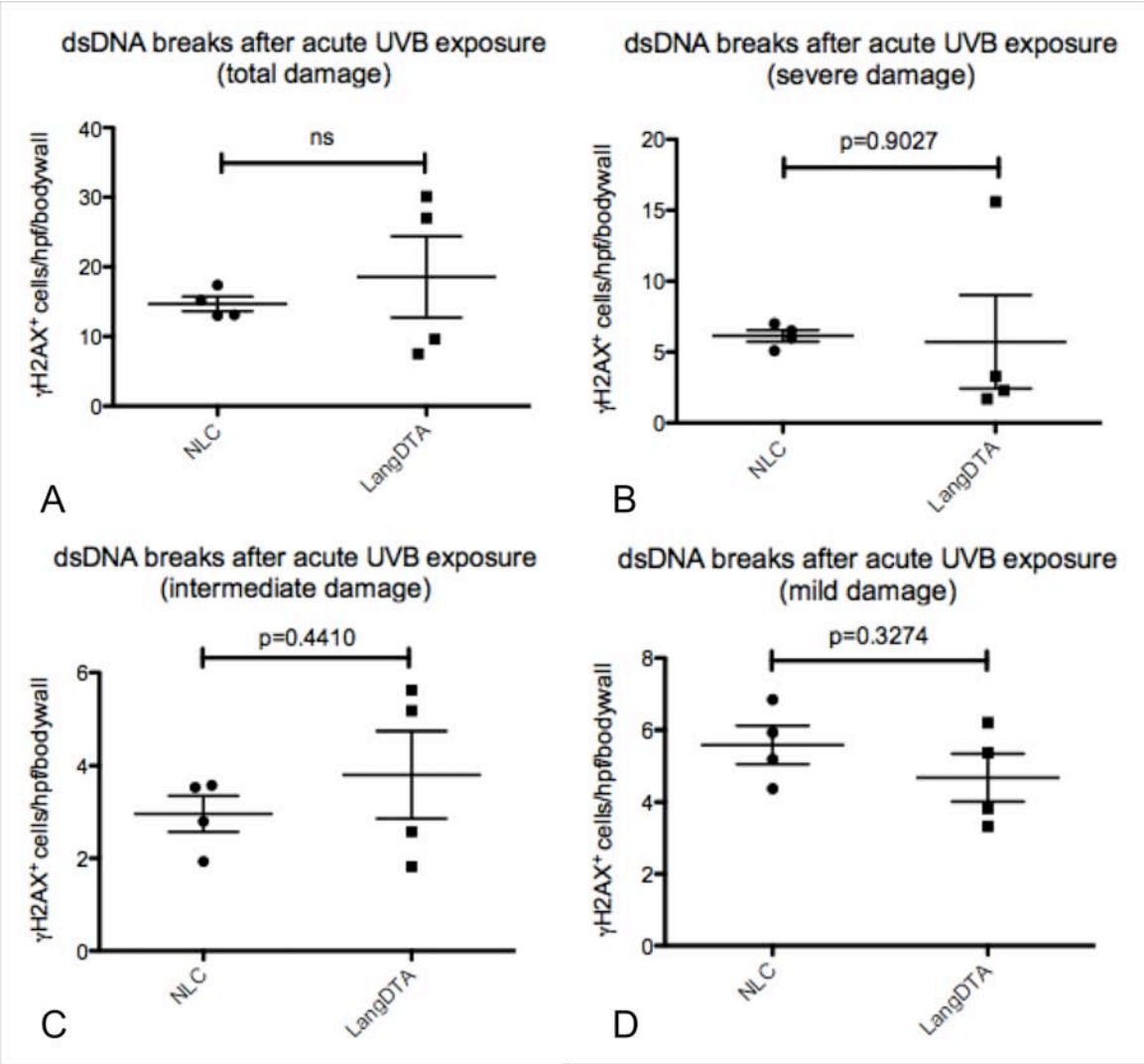


**Figure 13A: Effect of LC on UVB-induced dsDNA breaks assessed by the average γH2AX⁺ cells per hpf per mouse bodywall.** LangDTA and NLC dorsal bodywall was exposed to 50400 J/m$^2$ UVB irradiation, harvested immediately, and stained with γH2AX. Results were analyzed using the average number of γH2AX⁺ nuclei per hpf per mouse bodywall. Although there is no statistically significant difference, the trend for the total number of γH2AX⁺ nuclei shows an increase in LC-deficient epidermis. **(A)** total number of γH2AX⁺ nuclei per hpf per bodywall **(B)** number of nuclei with severe dsDNA damage per hpf per bodywall **(C)** number of nuclei with intermediate dsDNA damage per hpf per bodywall **(D)** number of nuclei with mild dsDNA damage per hpf results per hpf per bodywall

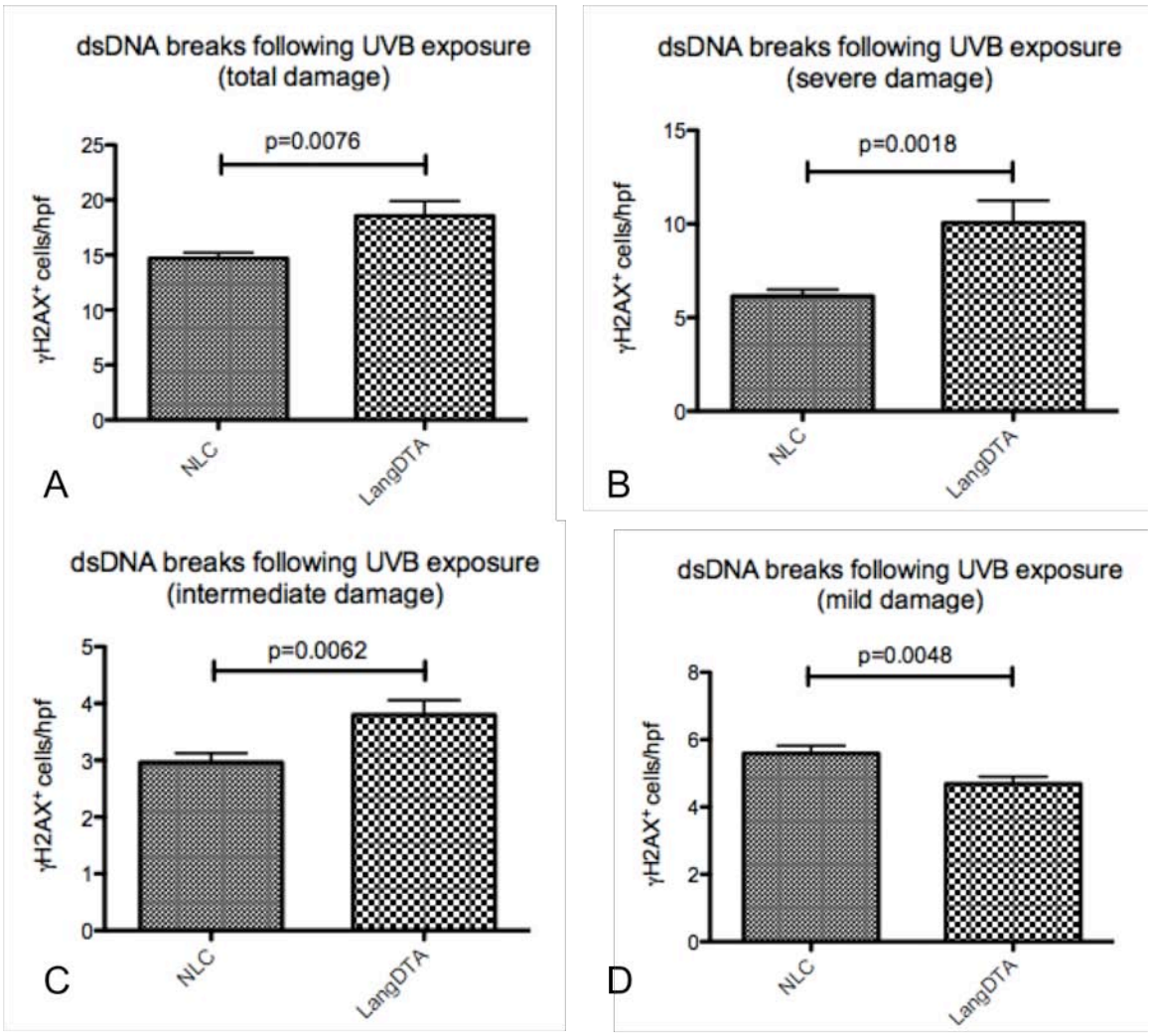


**Figure 13B: Effect of LC on UVB-induced dsDNA breaks assessed by γH2AX⁺ cells per hpf.** LangDTA and NLC dorsal bodywall was exposed to 50400 J/m$^2$ UVB irradiation, harvested immediately, and stained with γH2AX. Results were analyzed using the number of γH2AX⁺ nuclei per hpf. **(A)** total number of γH2AX⁺ nuclei per hpf **(B)** number of nuclei with severe dsDNA damage per hpf **(C)** number of nuclei with intermediate dsDNA damage per hpf **(D)** number of nuclei with mild dsDNA damage per hpf results per hpf

This experiment was repeated at an even lower UVB dose of 33600J/m$^2$ irradiation of dorsal epidermis to determine how large a dose of UVB exposure is necessary to appreciate a protective affect of LC on UVB-induced epidermal dsDNA breaks. There was an increase in the number of γH2AX$^+$ nuclei in LC-deficient (mean

24.45±3.1) compared to NLC (mean 23.85±3.3) murine epidermis, consistent with previous experiments, however the difference was not statistically significant, p=0.9 (Figure 14A,B). This suggests that this dose of UVB was not great enough to appreciate a difference using γH2AX staining.

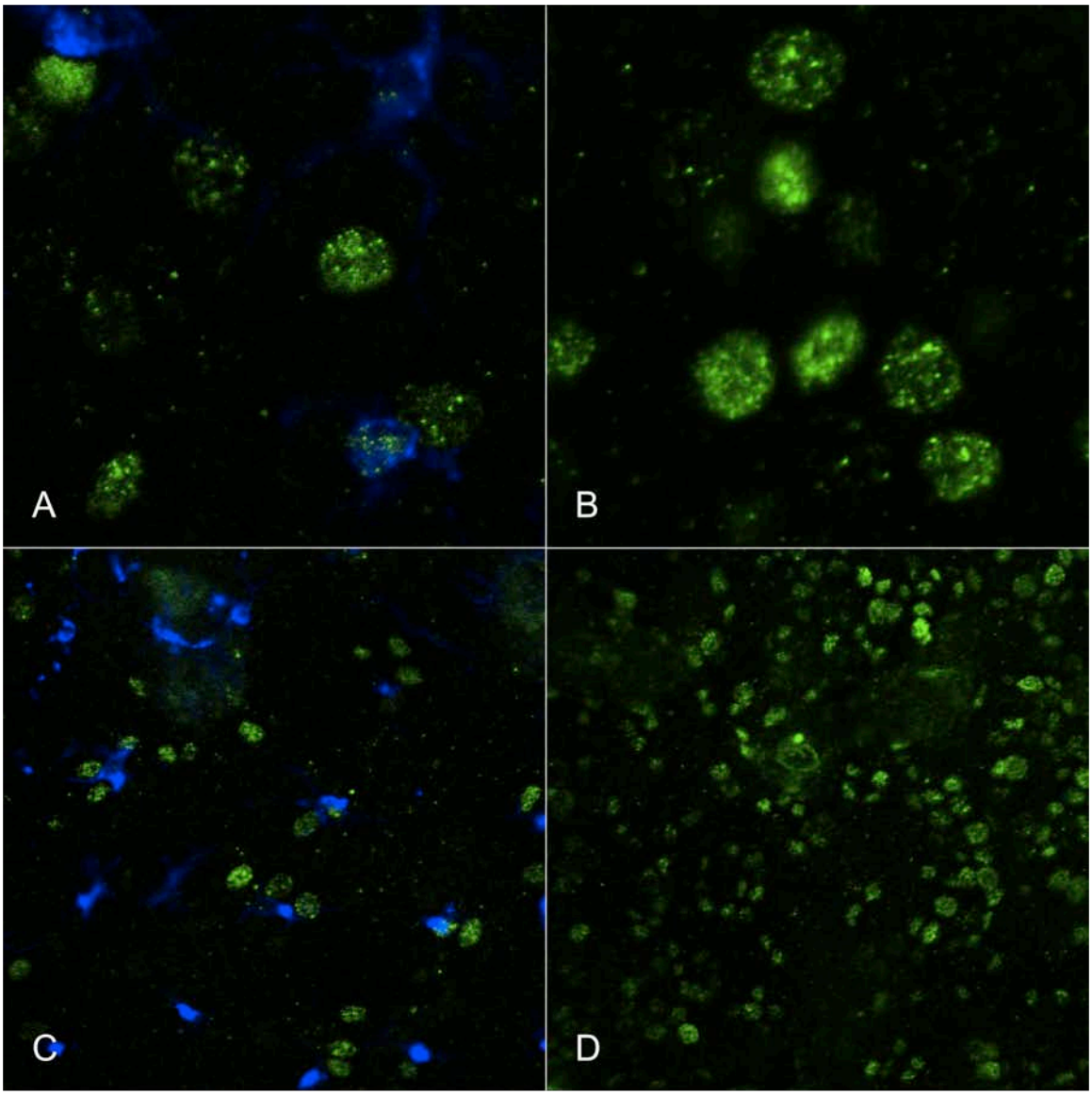


**Figure 14A: Epidermal sheets exposed to UVB irradiation.** LangDTA and NLC dorsal bodywall was exposed to 33600 J/m$^2$ UVB irradiation, harvested immediately, and stained for dsDNA breaks (green; γH2AX) and LC (blue;CD207). **(A)** NLC zoom view **(B)** LangDTA zoom view **(C)** NLC 63x magnification **(D)** LangDTA 63x magnification

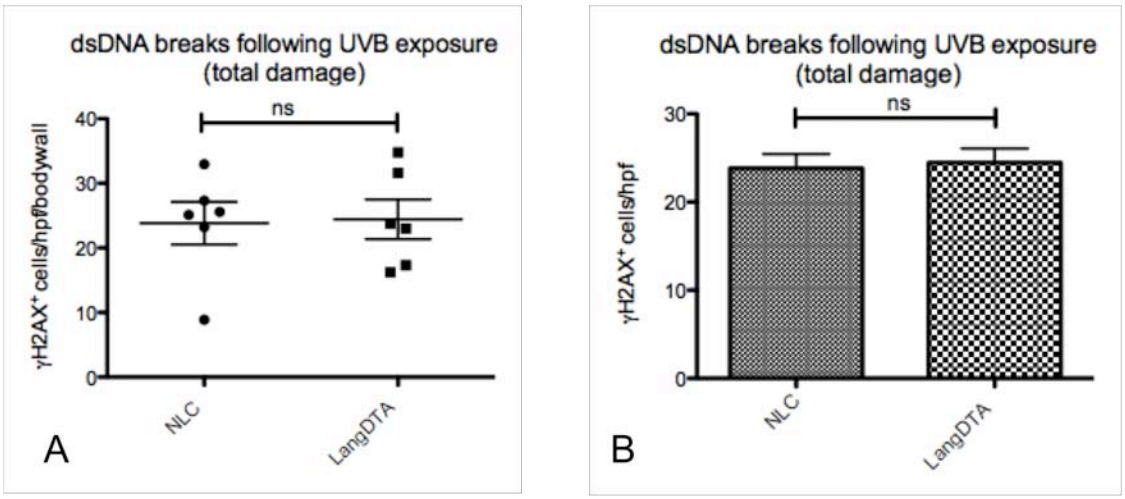


**Figure 14B: Effect of LC on UVB-induced dsDNA breaks.** LangDTA and NLC dorsal bodywall was exposed to 33600 J/m$^2$ UVB irradiation, harvested immediately, and stained with γH2AX. No statistically significant difference could be quantified at this dose of UVB irradiation. **(A)** total number of γH2AX$^+$ nuclei per hpf per bodywall **(B)** total number of γH2AX$^+$ nuclei per hpf

An attempt was made to assess the effect of chronic UVB exposure on LangDTA and NLC epidermis. Thirty-two ears were exposed to UVB for five weeks, five days a week, at an increasing dose from 5000 J/m$^2$ to 12500 J/m$^2$. Unfortunately, the antibody lot was non-specific and stained every cell nucleus as well as other cellular components; therefore, no useful data could be obtained (Figure 15). This is a potential hazard when using polyclonal antibodies. In the future, it may yield more consistent results to use a monoclonal γH2AX antibody.

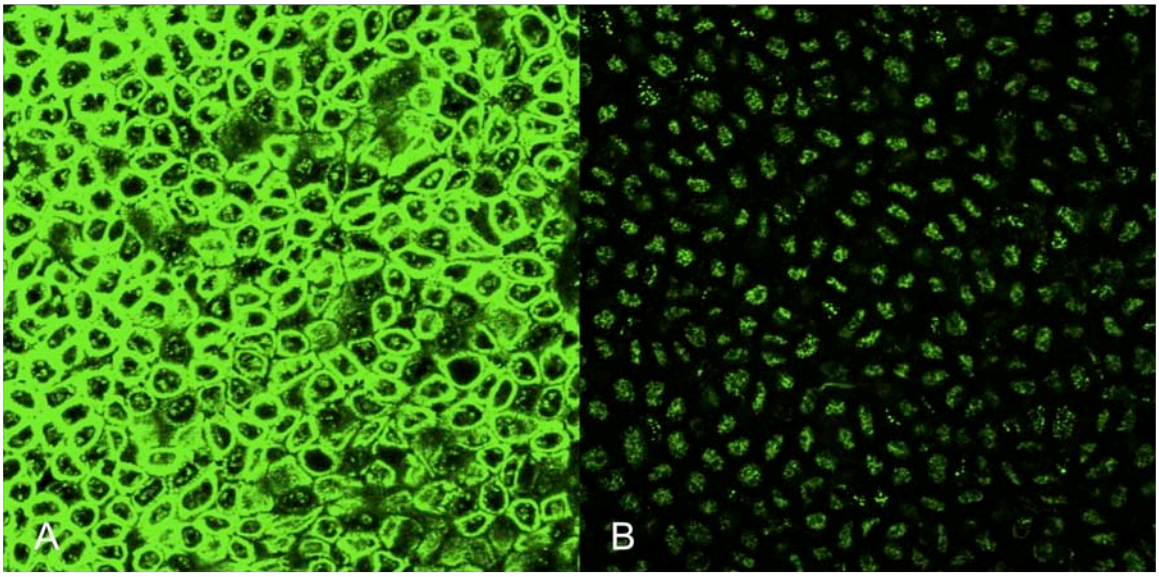


**Figure 15: Nonspecific γH2AX staining.** NLC and LangDTA ear epidermis was exposed to five days a week for five weeks of increasing UVB irradiation from 5000 to 12500 J/m$^2$. Ear epidermis was harvested one week after the last UVB dose and stained for dsDNA breaks (green; γH2AX). Unfortunately, the antibody lot was nonspecific. **(A)** non-histone cellular components staining γH2AX$^+$ **(B)** every nucleus staining γH2AX$^+$

## IV. Double-stranded DNA breaks in Chemically-induced Carcinogenesis

The role of LC in chemically-induced carcinogenesis is not understood. Therefore, we were interested in investigating the effect of LC on DMBA-induced DNA damage, specifically dsDNA breaks. We first compared DMBA-treated to non-treated controls in FVB mice to determine whether γH2AX staining could be used to quantify DMBA-induced dsDNA breaks. Depilated dorsal skin of FVB mice (n=12) was either treated with 0nmol or 400nmol of DMBA then harvested 24 hours later. The epidermis was stained with γH2AX to quantify dsDNA breaks as well as ToPro to mark the nuclei. The staining showed multiple punctate nuclear points, consistent with what would be anticipated for staining of histones at a specific site of dsDNA damage (Figure 16).

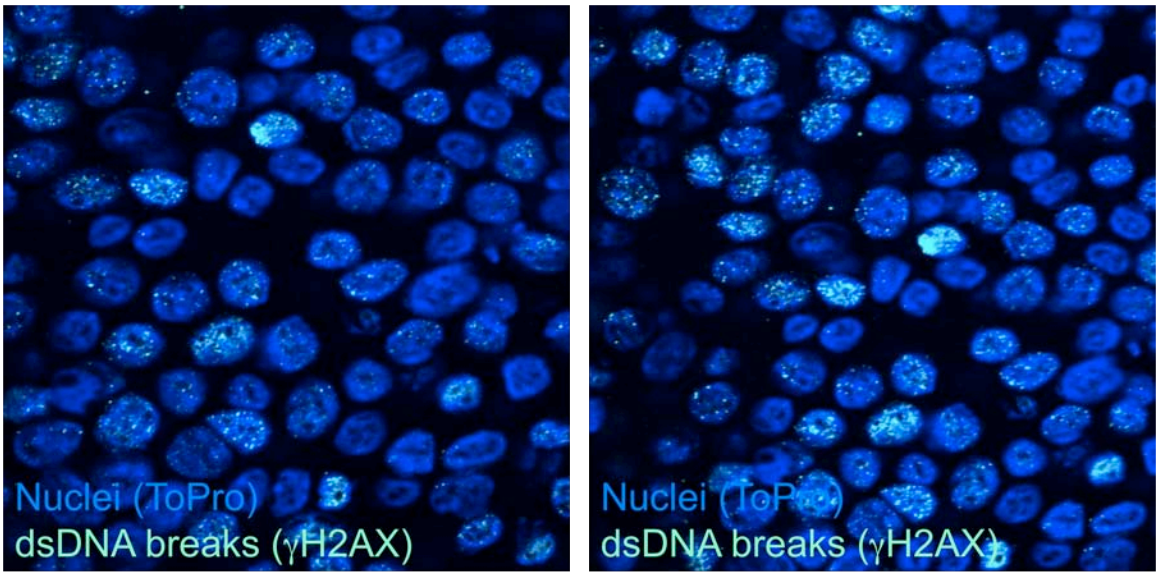


**Figure 16: γH2AX staining of DMBA exposed epidermal sheets.** FVB murine dorsal epidermis was exposed to 400 nmol of DMBA. Twenty-four hours after treatment, the epidermis was harvested and stained for dsDNA breaks.

The number of $\gamma H2AX^{+}$ nuclei in 20 consecutive 63x fields was quantified using epidermal sheets from the middle of the dorsum (along the spine) as we suspected that the most even DMBA application would be in this area. There was a statistically significant increase in the number of nuclei with dsDNA breaks in the DMBA treated epidermis (16.35±5.04) compared to the untreated epidermis (4.04±0.7), p=0.017 (Figure 17A-C). These results demonstrate the γH2AX staining can be used to assess DMBA-induced epidermal DNA damage; therefore we were in a position to use this method to investigate the role of LC.

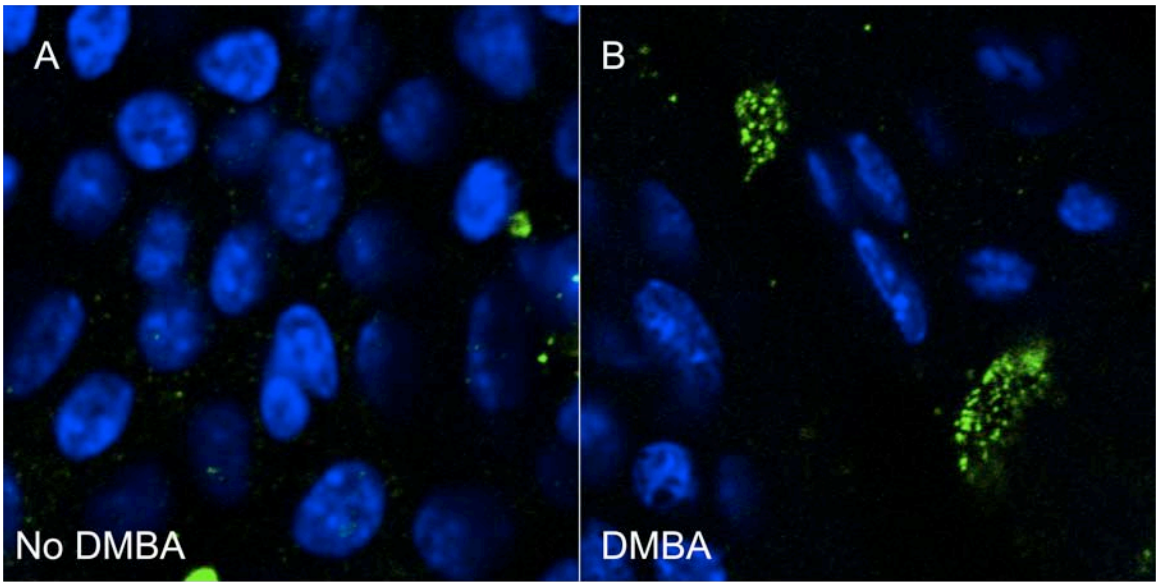


**Figure 17A: Epidermal sheets exposed to DMBA.** FVB murine dorsal epidermis was exposed to 0 or 400 nmol of DMBA. Twenty-four hours after treatment, the epidermis was harvested and stained for dsDNA breaks (green; γH2AX) and nuclei (blue; ToPro) **(A)** 0 nmol DMBA treated epidermis **(B)** 400 nmol DMBA treated epidermis

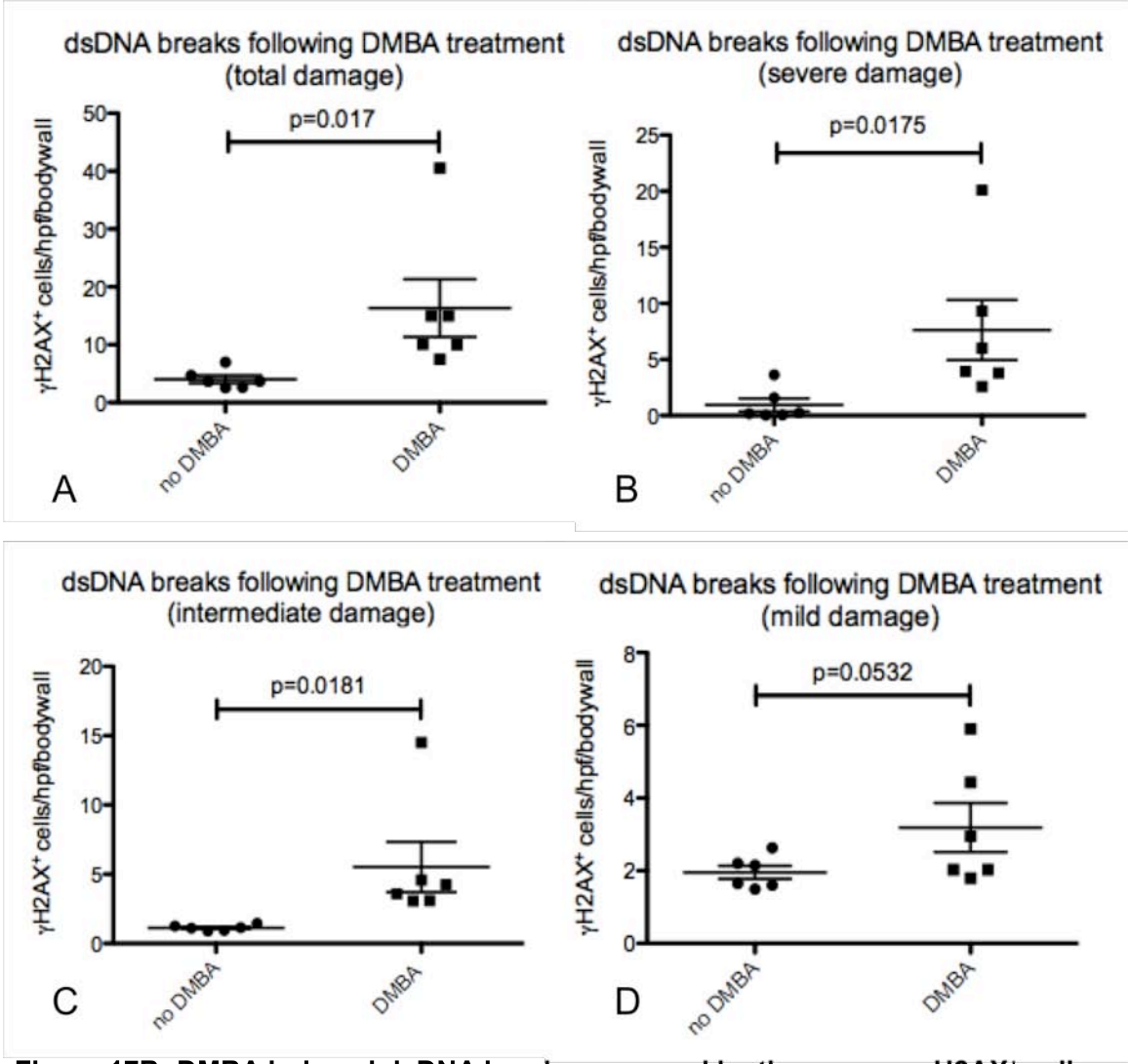


**Figure 17B: DMBA induced dsDNA breaks assessed by the average γH2AX⁺ cells per hpf per mouse bodywall.** FVB murine dorsal epidermis was exposed to 0 or 400 nmol of DMBA. Twenty-four hours after treatment, the epidermis was harvested and stained for dsDNA breaks. The average number of γH2AX⁺ nuclei per hpf per mouse bodywall was quantified. **(A)** total number of γH2AX⁺ nuclei per hpf per bodywall **(B)** number of nuclei with severe dsDNA damage per hpf per bodywall **(C)** number of nuclei with intermediate dsDNA damage per hpf per bodywall **(D)** number of nuclei with moderate dsDNA damage per hpf per bodywall

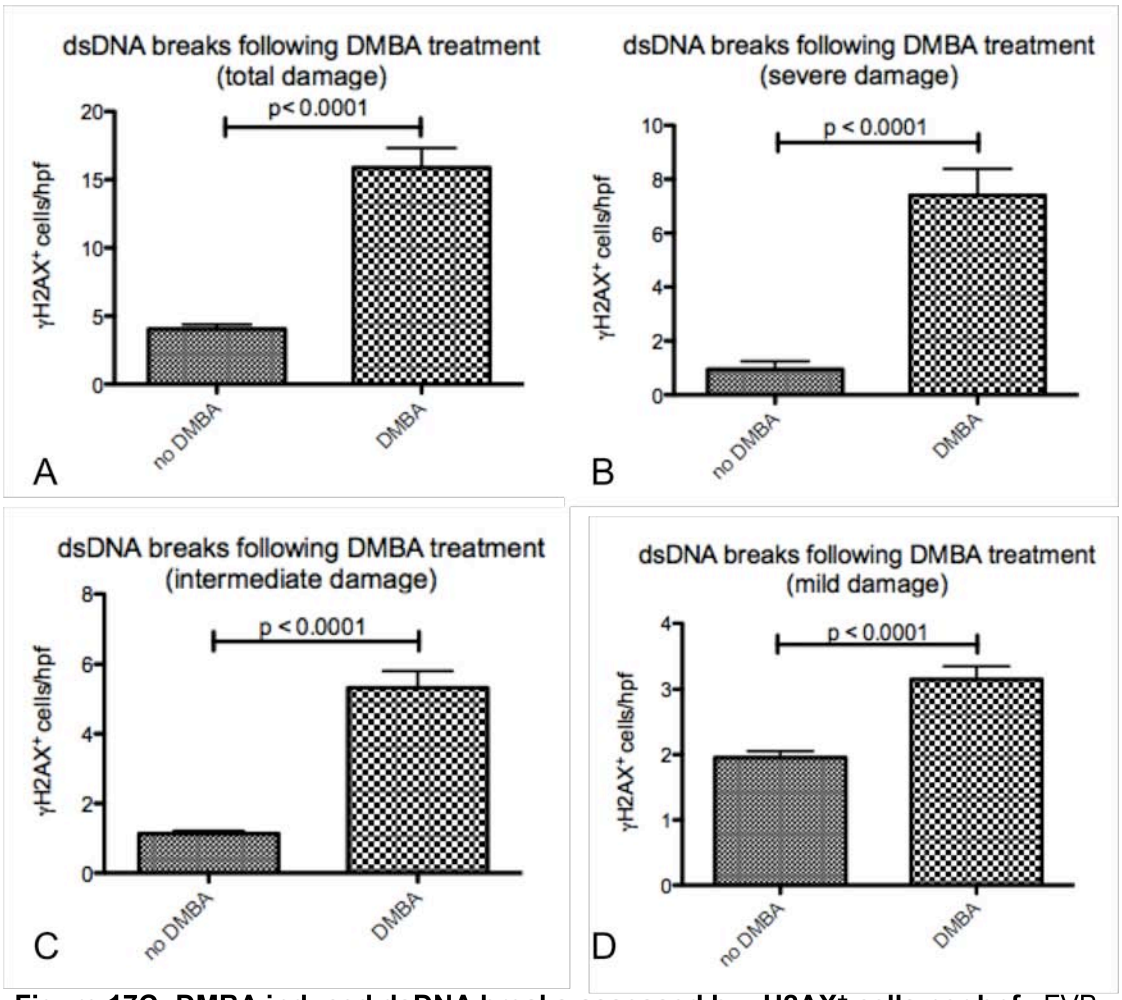


**Figure 17C: DMBA induced dsDNA breaks assessed by γH2AX+ cells per hpf.** FVB murine dorsal epidermis was exposed to 0 or 400 nmol of DMBA. Twenty-four hours after treatment, the epidermis was harvested and stained for dsDNA breaks. The number of γH2AX+ nuclei per hpf was quantified. **(A)** total number of γH2AX+ nuclei per hpf **(B)** number of nuclei with severe dsDNA damage per hpf **(C)** number of nuclei with intermediate dsDNA damage per hpf **(D)** number of nuclei with moderate dsDNA damage per hpf

huLangDTR mice allow the selective depletion of LC at a specific time point through the injection of diphtheria toxin (DT). This is a useful model to determine whether LC effect initiation or progression of cancer. To investigate whether this mouse model would be useful for assessing DNA damage using γH2AX staining, we compared DMBA-treated epidermis to non-treated controls in huLangDTR mice. LC were depleted

from 5 huLangDTR mice by intra-peritoneal injection of 400ng of DT. This amount of DT is two times the dose required to deplete LC from the epidermis, however less than half the dose required to deplete LC in the lymph nodes (1000ng). Therefore, we felt confident that the vast majority of LC in the epidermis were depleted. Viewing the epidermis in the confocal microscope verified that there were very few, if any LC remaining in the epidermis. The depilated dorsal skin of these huLangDTR mice and 5 NLC controls were treated with 400nmol of DMBA and sacrificed 24 hours later. The number of $\gamma H2AX^+$ cells per hpf as well as the average number of $\gamma H2AX^+$ cells per hpf per mouse bodywall were quantified. There was a trend toward decreased dsDNA breaks in LC-deficient epidermis, but no significant difference between NLC (mean 75.14±10.1) and huLangDTR (mean 63.84±7.2), $p>0.05$ when the average per hpf per mouse was used for assessment. However, there was a statistically significant decrease in dsDNA breaks in huLangDTR mice (62.82± 3.0) compared to NLC controls (81.15± 3.8), $p=0.0002$ when the results were assessed per hpf due to the greater *n* (Figure 18A-C). These results suggest that in this model, LC may enhance DMBA-induced DNA damage.

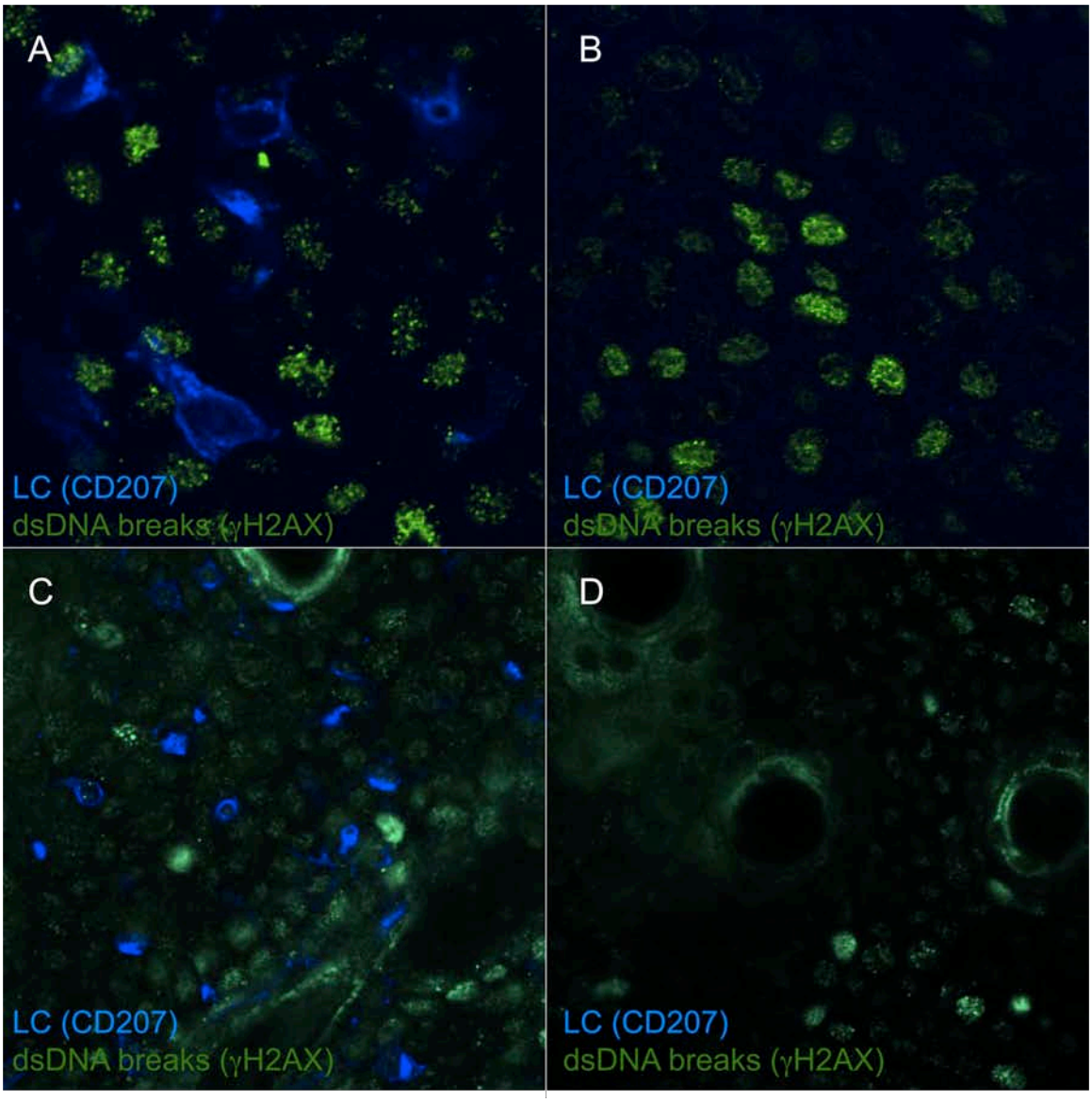


**Figure 18A: Epidermal sheets exposed to DMBA.** huLangDTR mice were injected with 400 ng DT. Twenty-four hours later, the huLangDTR and NLC dorsal skin was exposed to 400 nmol DMBA. The bodywalls were harvested 24 hours after DMBA treatment. **(A)** NLC zoom view **(B)** huLangDTR zoom view **(C)** NLC 63x magnification **(D)** huLangDTR 63x magnification

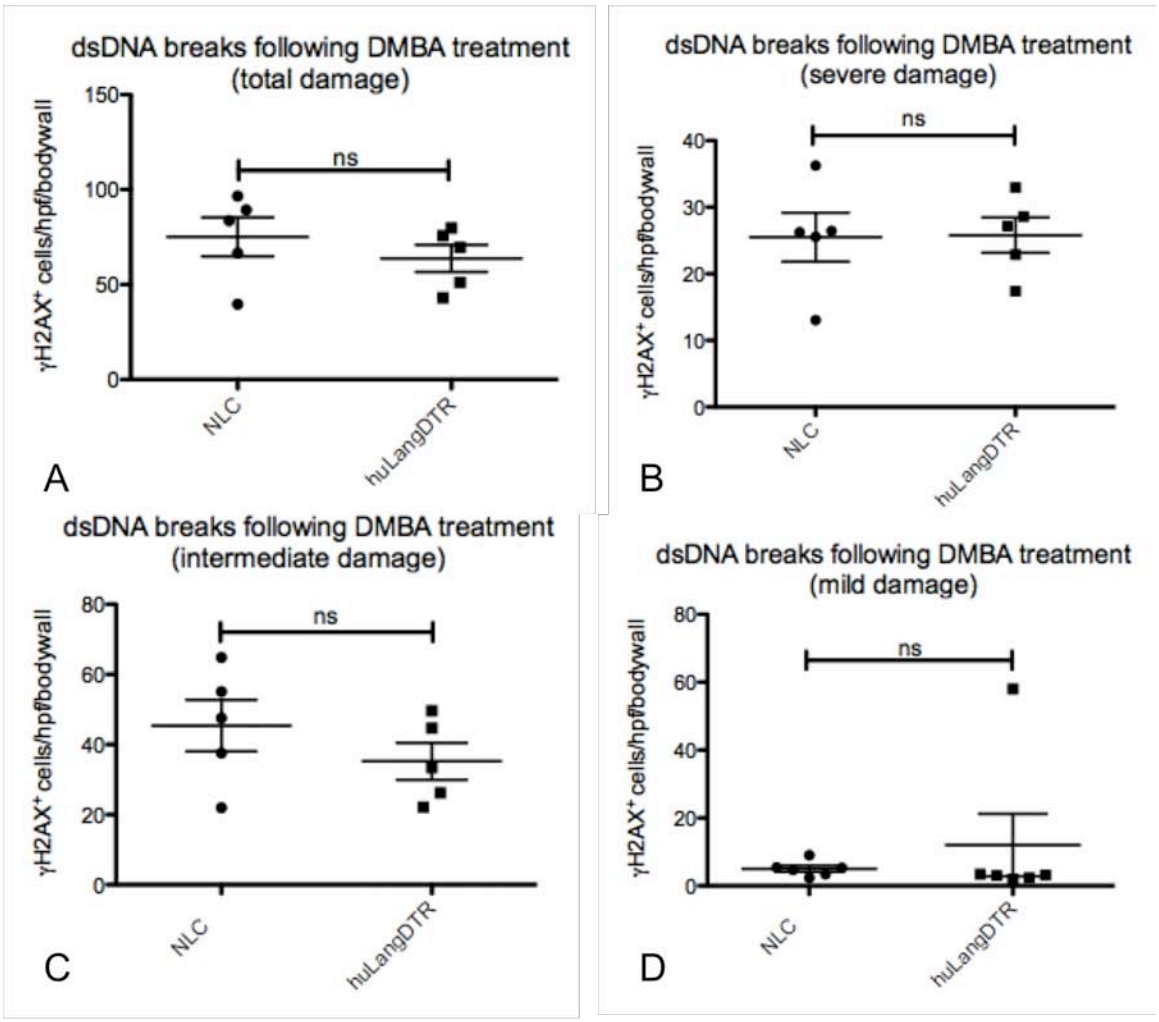


**Figure 18B: Effect of LC on DMBA-induced dsDNA breaks assessed by the average γH2AX⁺ cells per hpf per mouse bodywall.** huLangDTR mice were injected with 400 ng DT. Twenty-four hours later, the huLangDTR and NLC dorsal skin was exposed to 400 nmol DMBA. The bodywalls were harvested 24 hours after the DMBA treatment Results were analyzed using the average number of γH2AX⁺ nuclei per hpf per mouse bodywall. Although there is no statistically significant difference, the trend for the total number of γH2AX⁺ nuclei shows a decrease in LC-deficient epidermis. **(A)** total number of γH2AX⁺ nuclei per hpf per bodywall **(B)** number of nuclei with severe dsDNA damage per hpf per bodywall **(C)** number of nuclei with intermediate dsDNA damage per hpf per bodywall **(D)** number of nuclei with mild dsDNA damage per hpf results per hpf per bodywall

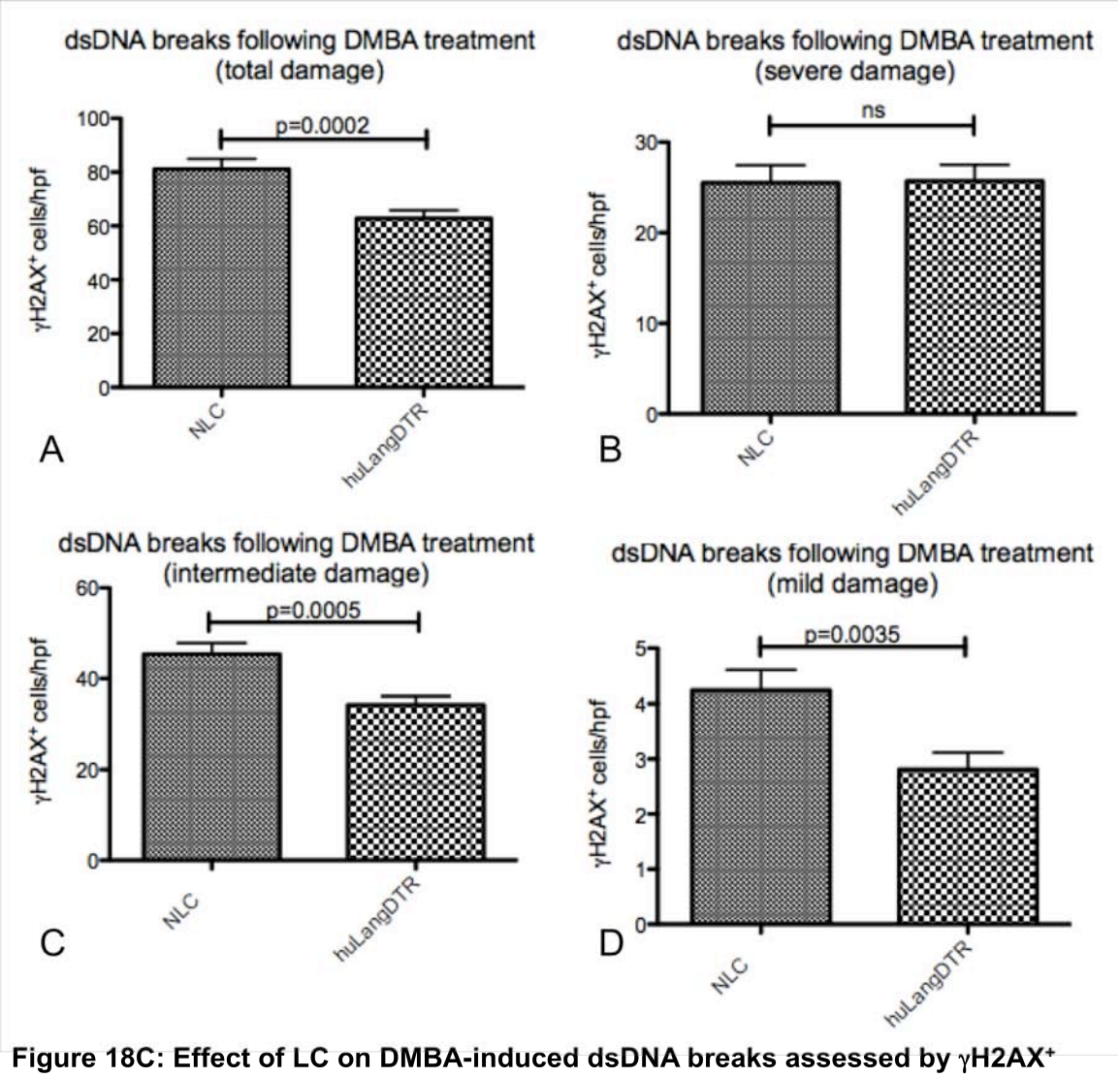


**Figure 18C: Effect of LC on DMBA-induced dsDNA breaks assessed by γH2AX⁺ cells per hpf.** huLangDTR mice were injected with 400 ng DT. Twenty-four hours later, the huLangDTR and NLC dorsal skin was exposed to 400 nmol DMBA. The bodywalls were harvested 24 hours after the DMBA treatment. Results were analyzed using the number of γH2AX⁺ nuclei per hpf. There was a statistically significant decrease in dsDNA breaks in the LC-deficient epidermis. **(A)** total number of γH2AX⁺ nuclei per hpf **(B)** number of nuclei with severe dsDNA damage per hpf **(C)** number of nuclei with intermediate dsDNA damage per hpf **(D)** number of nuclei with mild dsDNA damage per hpf

An attempt was made to assess the effect of longer-term DMBA and TPA exposure on dsDNA breaks in LangDTA mice compared to NLC. Depilated dorsal epidermis was exposed to 400nmol of DMBA, (n=16). One week later, 20nmol of TPA

was applied two times per week for seven total applications. Twenty consecutive 63x fields along the spine were assessed for γH2AX$^{+}$ cells. Regrettably, the lot of γH2AX antibody was nonspecific and reliable results could not be quantified. An experiment with this design would be informative to repeat, potentially with a monoclonal antibody, which would be more consistent than the polyclonal antibody used here (Figure 19).

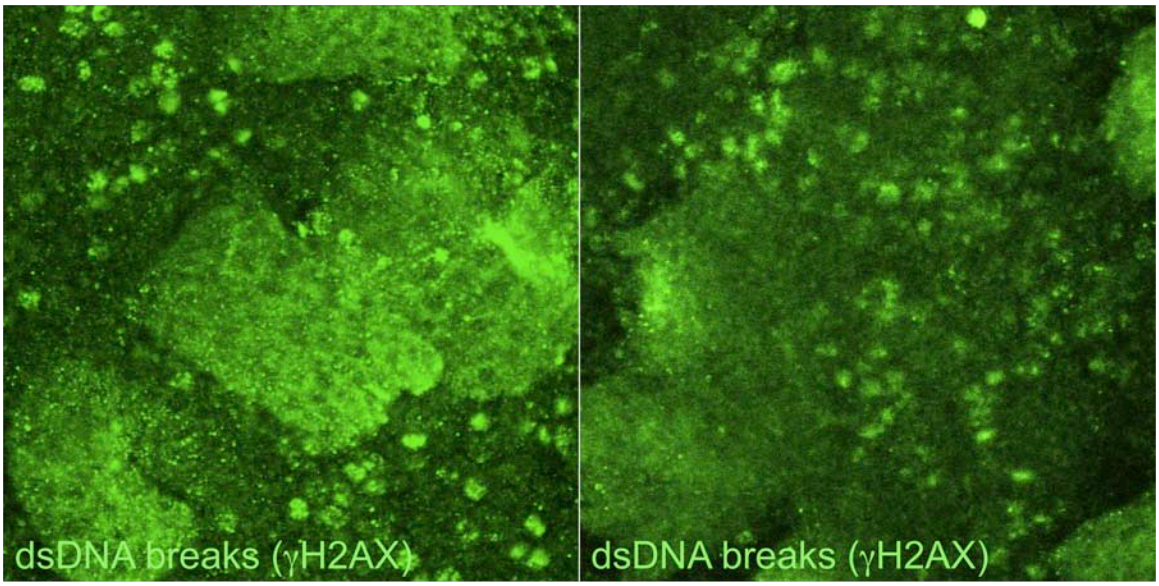


**Figure 19: Nonspecific γH2AX staining.** LangDTA and NLC dorsal epidermis was exposed to one dose of 400 nmol DMBA followed a week later by seven applications of 20 nmol TPA administered two times per week. The γH2AX antibody was nonspecific and stained every cell nucleus as well as other epidermal components.

## Discussion

### I. UVB-induced Oxidative Stress

These experiments are the first to describe the use of 8oxoguanine (8oxoG) immunofluorecent (IF) staining of epidermal sheets as an assay for assessing UVB-induced oxidative stress. IF staining with 8oxoG created a granular, cytoplasmic appearance, consistent with specific staining of ribosomal oxidized guanine. This is the anticipated staining pattern as the nuclei of the cells were not permeabilized (this would have required an acid or base, both of which may have increased background levels of oxidative stress). Additionally controls, including mouse IgM (an isotype-matched control) created a very different, diffuse stain, further indicating that the 8oxoG antibody was specific. All cells, including keratinocytes, LC, and T-cells exhibited 8oxoG staining following UVB irradiation, demonstrating that they are all susceptible to UVB-induced oxidative stress.

To assess the feasibility of using 8oxoG to quantify UVB-induced epidermal oxidative stress in our experimental model, we compared the intensity of 8oxoG staining of dorsal epidermis of FVB mice treated with increasing levels of UVB irradiation. There was a dose-dependent increase in UVB-induced levels of 8oxoG reaching statistical significance at 33600J/$m^2$ compared to un-irradiated skin. This is a high dose of UVB compared to doses used by Zhang, *et al*. A high dose or UVB was needed, however to overcome background levels of oxidative stress induced by epidermal sheet processing.

We were unsure whether the need to depilate and shave dorsal skin of mice would

affect results as depilatory cream and shaving induce epidermal irritation and an immure reaction, uneven hair removal, and potentially other changes. For this reason, skin was allowed to recover for one week between Nair application and shaving before UVB exposure. However, we could not rule out that this may have still caused unaccounted for changes in the epidermis. Furthermore, these experiments had to take place during resting hair growth (telogen stage), which occurs at 3 and 7 weeks of age in mice. Certain mice in an experiment may enter telogen earlier or later or have a more patchy hair distribution, therefore creating additional confounding factors. Hair follicles stain nonspecifically and although random fields were used, an uneven number of hair follicles could potentially skew data. Furthermore, the curved, rather than flat shape of the murine dorsum may cause the sides to receive less radiation than the middle when exposed to an overhead UVB bulb.

Using ear skin rather than dorsal skin allows completion of the experiment without Nair or shaving and ears may be taped flat for even UVB exposure. However, ears are more sensitive than dorsal skin and are subject to continuous small traumas due to their location sticking out from the side of the head. In addition, they provide less surface area for study.

Comparing un-irradiated ears to ears irradiated at 33600J/$m^2$ reinforced the findings of the prior dorsal skin experiment. There was a statistically significant increase in the intensity of 8oxoG in UVB-irradiated compared to un-irradiated skin.

The results of these preliminary experiments allowed us to feel confident in using 8oxoG IF to examine the effect of LC on UVB-induced oxidative stress. We compared LangDTA and normal littermate control (NLC) ear epidermal skin after exposure to

33600J/$m^2$ of UVB irradiation. There was an increase in the level of oxidative stress in the LC-deficient mice. These results suggest that LC may, in fact, be protective against UVB-induced keratinocyte oxidative stress. We then looked to see if T-cells may influence this phenomenon by comparing $\beta^{-/-}\delta^{-/-}$LangDTA mice to $\beta^{-/-}\delta^{-/-}$NLC (these mice lack all T-cells). Following exposure to 33600J/$m^2$ of UVB irradiation, we again found an increase in levels of oxidative stress in the LC-deficient mice. Thus demonstrating that LC appear to protect against UVB-induced keratinocyte oxidative stress in a T-cell independent manner.

Immune cells, including LC, are known to cause oxidative stress, so it is intriguing that the LC appear to protect against UVB-induced oxidative stress. Potentially, LC have a modulating effect on other immune cells. LC may also physically protect keratinocytes from UVB irradiation. A further possibility is that LC produce protective antioxidants. Further investigation into this phenomenon may have implications for cancer prevention.

When quantifying 8oxoG levels, we noticed a decrease in the number of LC present in FVB epidermis following UVB irradiation. LC have been shown to migrate out of the epidermis and undergo apoptosis following UVB irradiation (11), but the potential role of oxidative stress in this phenomenon is not known. We compared the percent of 8oxoG$^+$ LC per high power field (hpf) remaining in the epidermis after UVB irradiation to unexposed epidermis and found no difference. It is possible that many of the LC that migrated out of the epidermis (and therefore could not be seen in epidermal sheets) had high levels of oxidative stress, but could not be quantified. These findings appear to be independent of T-cells as UVB treated $\beta^{-/-}\delta^{-/-}$NLC epidermis produced

similar results: a statistically significant decrease in the number of LC present after UVB irradiation but no significant difference in the percent of 8oxoG$^+$ LC between the two groups.

Despite the increase in 8oxoG staining following UVB irradiation, there was high background oxidative stress in even un-irradiated epidermis. This is likely due to processing. For dorsal skin, using Nair to depilate the fur may increase background. All epidermal sheets were processed using EDTA, a reactive oxygen species producing chemical, to allow separation of the epidermis from the dermis. We attempted to eliminate the need for exposing the epidermis to EDTA by making frozen sections. However, these resulted in greater levels of nonspecific staining and were impossible to cut entirely parallel to the epidermis, thus providing varying areas for quantification. Furthermore, the amount of epidermis available for analysis was too small with this method. We also attempted to fix the skin before separating the epidermis from the dermis, therefore not exposing the epidermis to EDTA until it had been fixed. This resulted in an uneven separation of the skin layers, however, which was not optimal.

**II. Chemically-induced oxidative stress**

We were interested in using 8oxoG to assess oxidative stress caused by DMBA and TPA, the chemicals used to induce and promote skin cancer in previous experiments in the Girardi lab. TPA is an inflammatory agent, and therefore, is expected to produce high levels of oxidative stress. To test the feasibility of using 8oxoG to measure TPA-induced oxidative stress, ear skin of FVB mice was exposed to either the same level of TPA used in cancer-promotion, or no TPA. The results showed no statistically

significant difference. We were surprised by this result as we expected TPA to induce high levels of oxidative stress. Therefore, we increased the concentration of TPA by four times and applied two doses of TPA twenty-four hours apart. The first dose was expected to induce an immune response, causing free-radical-producing immune cells to immigrate to the epidermis so that there would be an increased response to the second dose of TPA. We used dorsal skin because the ears are more sensitive and may have started to erode with this high level of TPA exposure. Again, there was no statistically significant difference in the levels of 8oxoG between the treated and untreated skin.

Our inability to quantify a difference in the level of oxidative stress using 8oxoG IF between TPA treated and untreated epidermis may have been due to the high background created by the processing of epidermal sheets.

**C. UVB-induced Double Stranded DNA breaks**

These experiments represent a novel definitive assay for the assessment of UVB-induced double stranded DNA (dsDNA) breaks using γH2AX IF staining in epidermal sheets. To assess the feasibility of quantifying UVB-induced dsDNA breaks (DSB) using γH2AX, the number of $\gamma H2AX^+$ cells per hpf was compared between 33600 J/$m^2$ UVB exposed and unexposed FVB dorsal skin. There was a statistically significant increase in the number of cells per hpf with DSB as assessed by γH2AX after UVB exposure, demonstrating that γH2AX staining could be used to quantify UVB-induced epidermal DSB. We did not think that DSB would be induced by Nair application or shaving, so this initial experiment was done on dorsal skin rather than ears. However, there were still concerns that shaving may be uneven, hair follicles may affect the ability to accurately

count γH2AX$^+$ cells, and UVB exposure may be uneven due to the curved shape of the dorsum.

We compared the number of UVB-induced DSB in LangDTA and NLC in both dorsal and ear skin. Investigating a high dose of UVB (67200J/m$^2$) on ear skin resulted in a significant increase in DSB in LC-deficient epidermis. The ear skin is more fragile than dorsal skin and was difficult to handle after a high dose of UVB irradiation. Therefore, dorsal skin may be a better model for high-dose investigations; however, ears may display more subtle affects. This experiment was repeated at a lower dose (50400 J/m$^2$) on dorsal epidermis. The level of DNA damage was assessed as mild, moderate or severe to allow differentiation between nuclei with only one or few DSB, which may represent normal cell upkeep and damage, verses cells with moderate DSB that may be UVB induced, and cells with a large number of nuclear DSB, which may be undergoing mitosis with crossing over or apoptosis. The most accurate results appeared to be the total number of DSB as the classifications were subjective. The results again demonstrated a higher level of DSB in LC-deficient epidermis. A third experiment using dorsal skin at an even lower dose of UVB (33600 J/m$^2$) did not show any difference, suggesting that this assay is not sensitive enough to pick up differences at lower doses of UVB exposure. The development of a more sensitive test would be helpful as the amount of UVB irradiation at which differences in LC-deficient epidermis can be quantified are very high compared to the doses humans would be exposed to under normal circumstances from the sun.

We also pursued a chronic UVB experiment in which mice received five weeks of treatment five days a week of an increasing dose of UVB from 5000 to 12500 J/m$^2$.

Unfortunately, the γH2AX antibody lot used was non-specific and stained every cell nucleus as well as other cellular components. Therefore, no useful results could be obtained. This is a hazard of using polyclonal antibodies. In the future, it would be advantageous to repeat this experiment with a monoclonal γH2AX antibody.

**IV. Chemically-induced Double Stranded DNA breaks**

The carcinogenic effects of DMBA are brought about by DNA damage and mutations, specifically in the oncogene, Ras. We developed a novel assay for assessing dsDNA breaks in epidermal sheets using γH2AX IF staining. To assess the feasibility of quantifying DMBA-induced DNA damage by γH2AX staining, we applied 400nmol of DMBA to the backs of FVB mice and compared the number of $\gamma H2AX^+$ cells per hpf to unexposed controls. There was a statistically significant increase in the number of $\gamma H2AX^+$ cells per hpf in the skin treated with DMBA compared to untreated skin. Furthermore, co-staining with the nuclear marker, ToPro showed that the γH2AX staining was indeed nuclear as would be expected and the punctate pattern was consistent with marking specific histones. Therefore, we felt confident that this method could be used to quantify a possible LC-dependent difference in DMBA-induced DSB.

As there were no LangDTA mice available at the time this experiment was planned, huLangDTR mice were used as LC-deficient mice. There are advantages and disadvantages to both strains. LangDTA are advantageous in that there is an absolute LC deficiency that is consistent from mouse to mouse and no need to inject diphtheria toxin, which may have toxic and immunogenic affects. huLangDTR mice are advantageous in that because LC are present during development, we are assured that there are no

unaccounted for changes in the development of the epidermis due to lack of LC during growth and differentiation. Furthermore, LC can be eliminated at different time-points, thus allowing more specific experiments observing the role of LC. However, the injection of diphtheria toxin does not completely knock out all LC and the level of LC deficiency is variable between mice. Furthermore, the death of LC after diphtheria injection may affect surrounding cells.

huLangDTR and NLC dorsal skin was exposed to 400nmol of DMBA and stained with γH2AX to assess DSB. There was a decrease in the number of DSB per hpf in the LC-deficient epidermis compared to NLC. This suggests that LC may somehow contribute to DMBA-induced DNA damage. The mechanism is unknown, however there may be a soluble factor secreted from LC that affects neighboring keratinocytes.

A longer-term experiment was attempted in which mouse dorsal skin was painted with one dose of 400nmol of DMBA followed by 7 doses of 20nmol of TPA over 4 weeks. However, the antibody lot of γH2AX used was non-specific and stained every cell nucleus as well as other cellular components. Therefore, no useful results could be obtained. A repeat of this experiment using a monoclonal antibody should be pursued.

**V. Future Directions**

To avoid the problems faced with depilatory cream, shaving, and uneven hair growth, hairless mice are being bred onto the FVB/LangDTA and FVB/huLangDTR backgrounds. These mice would allow experiments to be repeated using dorsal skin with a significant decrease in confounding factors. Furthermore, repeated long-term UVB and chemical experiments should be pursued as carcinogenesis occurs over time, and the

results may be more applicable to human skin cancer. The huLangDTR strain of mouse will allow experiments with both 8oxoG and γH2AX to be performed with LC depleted after the initiation stage to assess their role specifically in promotion.

Future experiements using γH2AX IF should use a monoclonal antibody rather than a polyclonal antibody for more consistent and predictable staining. Co-staining of γH2AX with an apoptotic marker, such as caspase-3, would allow assessment of which cells with DNA damage are undergoing apoptosis. This may shed light on how LC are affecting damaged keratinocyte survival and whether the survival of damaged cells may be inducing cancer.

The role of LC in carcinogenesis is poorly understood and further investigation may have great implications in immunotherapy and even cancer prevention.

## References


1. Burnet, M. Immunological factors in the process of carcinogenesis. *Brit Med Bulletin.* 20:154-158. 1964.

2. Peto J. Cancer epidemiology in the last century and the next decade. *Nature.* 411(6835):390-5. 2001.

3. Girardi M, Glusac E, Filler R, Tigelaar R, Hayday AC. The distinct contributions of murine TCRab$^{+}$ and TCRgd$^{+}$ T cells to different stages of chemically-induced skin cancer. *J Exp Med.* 198(5):747-755. 2003.

4. Strid J, Roberts S, Filler R, Ng B, Kaplan D, Hayday AC, Girardi M. NKG2D-ligand upregulation promotes rapid reorganization of a local immune compartment with pleiotropic effects on carcinogenesis. *Nature Immunology.* 9(2):146-54. 2008.

5. Roberts S, Ng B, Filler R, Lewis J, Hayday AC, Tigelaar R, Girardi M. Characterizing tumor-promoting T cells in chemically induced cutaneous carcinogenesis. *Proc Natl Acad Sci U S A.* 104:6770-6775. 2007.

6. Kaplan DH, Jenison MC, Saeland S, Shlomchik WD, Shlomchik MJ. Epidermal langerhans cell-deficient mice develop enhanced contact hypersensitivity. *Immunity.* 23(6):611-20. 2005.

7. Nishibu A, Ward BR, Jester JV, Ploegh HL, Boes M, Takashima A. Behavioral responses of epidermal Langerhans cells in situ to local pathological stimuli. *J Invest Dermatol*. 126(4):787-96. 2006.

8. Kawanishi S, Hiraku Y, Oikawa S. Mechanism of guanine-specific DNA damage by oxidative stress and its role in carcinogenesis and aging. *Mutation Res*. 488:65-76. 2001.

9. Poirier M. Chemical-induced DNA damage and human cancer risk. *Nature Rev Cancer*. 4(8):630-637. 2004.

10. Finch JS, Albino HE, Bowden GT. Quantitation of early clonal expansion of two mutant 61$^{st}$ codon c-Ha-*ras* alleles in DMBA/TPA treated mouse skin by nested PCR/RFLP. *Carcinogenesis.* 17(12):2551-2557. 1996.

11. Mena S, Ortega A, Estrela J. Oxidative stress in environmental-induced carcinogenesis. *Mutation Res.* 674:36-44. 2009.

12. Mehrotra S, Mougiakakos D, Johansson C, Voelkel-Johnson C, Kiessling R. Oxidative stress and lymphocyte persistence: implications in immunotherapy. *Cancer Res.* Elsevier, Inc. 2009.

13. Federico A, Morgillo F, Tuccillo C, Ciardiello F, Loguerci C. Chronic inflammation and oxidative stress in human carcinogenesis. *Int. J. Cancer.* 121:2381-2386. 2007.

14. Kunisada M, Kunihiko S, Tominaga Y, Budiyanto A, Ueda M, *et al*. 8-oxoguanine formation induced by chronic UVB exposure makes Ogg1 knockout mice susceptible to skin carcinogenesis. Cancer Res. 65(14). 2005.

15. Zhang W, Hanks A, Boucher K, Florell S, Allen S, Alexander A, Brash D, Grossman D. UVB-induced apoptosis drives clonal expansion during skin tumor development. *Carcinogenesis.* 26(1):249-257. 2005.

16. Timares L, Katiyar SK, Elemts CA. DNA damage, apoptosis and Langerhans cells--activators of UV-induced immune tolerance. *Photochem Photobiol* 84(2):422-436. 2008.

17. Qureshi A, Hosoi J, Xu S, Takashima A, Granstein R, Lerner E. Langerhans cells express inducible nitric oxide synthase and produce nitric oxide. *J Invest Dermatol.* 107:815-821. 1996.

18. Staszewski O, Nikolova T, Kaina B. Kinetics of gH2AX focus formation upon treatment of cells with UV light and alkylating agents. *Envir & Mol Mut* 49:734. 2008.

19. Bonner W, Redon C, Dickey J, Nakamura A, Sedelnikova O, Solier S, Pommier Y. γH2AX and cancer. *Nature* 8:957. 2008.

20. Halicka H, Huang X, Traganos F, King M, Dai W, Darzynkiewicz Z. Histone H2AX phosphorylation after cell irradiation with UV-B. *Cell Cycle* 4(2):339. 2005.

21. Bennet, C.L., van Rijn E, Jung S, Unaba K, Steinman R, Kapsenbert M, *et al.* Inducible ablation of mouse Langerhnas cells diminishes but fails to abrogate contact hypersensitivity. *J Cell Biol* 169:569-576. 2005.